AFRL-VS-TR-2001-1608 VRISV-1130-AR02

Irradiance Calibration of Space-Based Infrared Sensors

Russell G. Walker
Martin Cohen

Vanguard Research, Inc.
5321 Scotts Valley Drive, Suite 204
Scotts Valley CA 95066

July 2000

Scientific Report No. 2

AIR FORCE RESEARCH LABORATORY
Space Vehicles Directorate
29 Randolph Rd
AIR FORCE MATERIEL COMMAND
Hanscom AFB, MA 01731-3010

"This technical report has been reviewed and is approved for publication"

/signed/

TAMILYN BECKER, 2/Lt, USAF
Contract Manager

/signed/

ROBERT BELAND
Branch Chief

This report has been reviewed by the ESC Public Affairs Office (PA) and is releasable to the National Technical Information Service (NTIS).

Qualified requestors may obtain additional copies from the Defense Technical Information Center (DTIC). All others should apply to the National Technical Information Service (NTIS).

If your address has changed, if you wish to be removed from the mailing list, or if the addressee is no longer employed by your organization, please notify AFRL/VSIM, 29 Randolph Road, Hanscom AFB MA 01731-3010. This will assist us in maintaining a current mailing list.

Do not return copies of this report unless contractual obligations or notices on a specific document require that it be returned.

REPORT DOCUMENTATION PAGE

Form Approved
OMB No. 0704-0188

1. AGENCY USE ONLY *(Leave blank)*	2. REPORT DATE	3. REPORT TYPE AND DATES COVERED
	July, 2000	Annual Interim Report #2 May 27, 1999 – May 30, 2000

4. TITLE AND SUBTITLE
Irradiance Calibration of Space-Based Infrared Sensors, Annual Report No. 2

5. FUNDING NUMBERS
C F19628-98-C-0047
PE 63871 C
PR MSX 8
TA BS
WU AE

6. AUTHORS
Russell G. Walker and Martin Cohen

7. PERFORMING ORGANIZATION NAME(S) AND ADDRESS(ES)
Vanguard Research, Inc.
5321 Scotts Valley Drive, Suite 204
Scotts Valley, CA 95066

8. PERFORMING ORGANIZATION REPORT NUMBER
VRISV-1130-AR02

9. SPONSORING/MONITORING AGENCY NAME(S) AND ADDRESS(ES)
Air Force Research Laboratory
29 Randolph Road
Hanscom AFB, MA 01731-3010
Contract Manager: Dale Sinclair, VSBT

10. SPONSORING/MONITORING AGENCY REPORT NUMBER
AFRL-VS-TR-2001-1608

11. SUPPLEMENTARY NOTES

12a. DISTRIBUTION/AVAILABILITY STATEMENT
Approved for Public Release; Distribution Unlimited.

12b. DISTRIBUTION CODE

13. ABSTRACT *(Maximum 200 words)*
The purpose of this work is to develop a basis for irradiance calibration of space-based infrared sensors. It is an extension of previous work that fully defines the context of the calibration, and the concepts of spectral composites and templates. We discuss four major accomplishments during the past year and our plans for the future. The accomplishments are:

1) Data from the MSX/SPIRIT III CB06 celestial background calibration experiments have been reduced, validated, and analyzed to produce a sub-network of calibration stars that are now integrated into the current calibration network.
2) The absolute calibration of the infrared radiometry of the MSX Point Source Catalog, Version 1.2 (PSC1.2) has been validated.
3) An Air Force Bright Spectral Catalog (AFBSC) Version 1 has been developed and delivered that offers a new set of spectral (2-35μm) irradiance calibrators selected from the IR-brightest sources in the sky.
4) ASTCAT Version 2.0 was completed and delivered to the PL DAC in support of the MSX Point Source Catalog.

14. SUBJECT TERMS
IR Sources, Calibration, Spectra, Stars, Asteroids

15. NUMBER OF PAGES
95

16. PRICE CODE

17. SECURITY CLASSIFICATION OF REPORT	18. SECURITY CLASSIFICATION OF THIS PAGE	19. SECURITY CLASSIFICATION OF ABSTRACT	20. LIMITATION OF ABSTRACT
UNCLASSIFIED	UNCLASSIFIED	UNCLASSIFIED	UL

Contents

Figures

Tables

1. INTRODUCTION

Satellites employing infrared sensors are continually being launched by space agencies such as NASA and ESA and by the US DOD community. The successes of IRAS, ISO, IRTS, and MSX have already produced enormous infrared databases. Consequently, there must now be greater emphasis on data verification, validation, and calibration issues to assure that these data sets are of sufficient reliability for application to the quantitative design of advanced spaceborne sensors and systems. There is an urgent need not only to rationalize infrared calibration and place it in a common and well-defined context, but also to provide a network of calibrators well distributed across the sky, with a common traceable pedigree. This network should be sufficiently populated to have a member relatively close to any arbitrary direction because satellites and aircraft cannot afford to slew through large angles to secure measurements of the few traditional calibration objects. Dynamic range, too, is an issue and such a network must include stars both fainter and brighter than today's popular "standards."

The purpose of this work is to develop a basis for irradiance calibration of space-based infrared sensors. It is an extension of previous work (Cohen, et al. Papers 1-9, 1992-1998) that fully defines the context of the calibration, and the concepts of spectral composites and templates. This work culminated in the recent publication of *An All Sky Network of 422 Infrared Calibration Stars* (Cohen, et al. 1999). Our approach is based on a self-consistent absolute framework within which radiometry and spectroscopy are unified, with wavelength coverage ideal for calibrating many satellite, airborne, and ground-based sensors.

During the past year our work was concentrated in three areas:

a) Data from the MSX/SPIRIT III CB06 celestial background calibration experiments were reduced, validated, and analyzed to produce a sub-network of calibration stars that was integrated into the previous network of 422 calibration stars. This sub-

network was used to provide an independent check on the internal consistency of the infrared spectral templates used in the network, as well as add several new stars to the network.

b) The absolute calibration of the infrared radiometry of the MSX Point Source Catalog, Version 1.2 (PSC1.2) was validated using two sets of calibration standards. The first was a subset of stars from the current all-sky network, while the second was a set of other stars that also support the ISO calibration.

c) Data from the literature were assembled and analyzed to produce an independent set of calibrators selected to be among the IR-brightest sources in the sky rather than sources selected by specific optical type. This Air Force Bright Spectral Catalog (AFBSC), Version 1, although limited in both scope and accuracy, is particularly relevant to space-based programs, such as SBIRS, and to ground-based programs in the 20 μm spectral region such as those to begin soon at AMOS using the new Air Force Laboratory 3.5 meter telescope.

This report describes the methods, assumptions, and procedures used to accomplish the above work; and then discusses work that will be pursued in the coming year.

2. CELESTIAL BACKGROUND EXPERIMENT CB06

The activities on the MSX Celestial Backgrounds Experiment, CB06, are discussed in detail in a preprint of *Spectral Irradiance Calibration in the Infrared. XII. Radiometric Measurements from the Midcourse Space Experiment (MSX)* that is included as Appendix A of this report, and that has been submitted to the MSX Program for approval and release. As soon as approval has been received, the paper will be submitted to the Astronomical Journal for publication. In Appendix A we describe the series of CB06 absolute stellar irradiance calibration experiments conducted by the Midcourse Space Experiment (MSX). These experiments validate the published absolute irradiances of our primary and secondary standards, namely α CMa and a set of bright K-M giant stars, and confirm their radiometric

"closure" (relative irradiances). We also validate the absolute spectra of 28 of the fainter calibrators that have been previously published and create additional faint reference stars from the MSX data. This work underpins the absolute calibrators provided for DIRBE, IRTS, ISO, our all-sky network of 422 fainter calibration stars (Cohen et al. 1999: Paper X), and the MSX Point Source Catalog, Version 1.2. There is no plan to pursue work on the CB06 data during the next year. Publication of the results will complete the effort.

3. RADIOMETRIC VALIDATION OF THE MSX POINT SOURCE CATALOG

Our methods and approach to validating the radiometric calibration of the MSX Point Source Catalog, Version 1.2 (PSC1.2) are given in detail in the preprint *Radiometric Validation of the Midcourse Space Experiment's (MSX) Point Source Catalogs & the MSX Properties of Normal Stars,* which is included as Appendix B of this report. This paper has been submitted to the Astronomical Journal for publication. In Appendix B we describe our methods to validate the absolute calibration of the infrared (IR) radiometry of the MSX Point Source Catalog, version 1.2 (PSC1.2). These are based upon stars drawn from our current all-sky network of absolute calibrators, and other stars that also support the calibration of ESA's Infrared Space Observatory (ISO) and of several other satellites. All four of MSX's mid-IR bands are entirely consistent with this network but the two narrowest bands (near 4.3 μm) are discrepant by a few percent. This paper probes radiometry of fainter stars than those validated by an independent study of the primary and secondary MSX standards by Cohen et al. (2000). To provide the user of the PSC1.2 with a basis for comparison, we derive the IR properties of normal stars from measurements by MSX's infrared focal planes. Publication of the above paper will complete the validation work on MSX PSC1.2. MSX PSC2 has now been released. There should be no differences in the radiometric calibration from that in PSC1.2 with the exception of SPIRIT III Band B. We anticipate that we will attempt to revalidate Band B as part of the next years effort.

4. THE AIR FORCE BRIGHT SPECTRAL CATALOG

The AFBSC is an independent set of calibrators selected to be among the IR-brightest sources in the sky. Our ultimate goal is to create complete (2-35 μm) spectra for all stars brighter than zero magnitude in the infrared.

AFBSC Version 1.0 is an extremely limited version that does not pretend to achieve the overall AFBSC goals either in quantity or quality of the sources. It is a result of an initial "testing of the waters" and serves a number of useful purposes. It alerts the systems designer to the potential bright calibrators that will be available to him for calibration of his spacebased, groundbased, and airborne IR systems. The irradiance levels and dynamic range possible are well-defined, even though many absolute irradiance levels have, at present, unacceptably large uncertainties for radiometric calibration. Many of these will still be useful astrometric calibrators and knowing the range of their irradiances will improve infrared acquisition by enabling discrimination among multiple objects in the field. Furthermore, many stars are identified in this version that do have reliable and non-varying irradiances with acceptable uncertainties, and are immediately applicable for radiometric calibration. Finally, production of this version of the catalog has identified to the authors those stars that can be readily elevated to precise calibration status, and those that will require gargantuan efforts. The AFBSC Version 1 consists of 1118 ASCII files, one for each cataloged star, plus an Explanatory Supplement. The catalog embodies 116 non-variable stars of which 35 are previously published "standards", 66 are K III stars, and 1002 are variable stars. Thirty-five stars from our previously published models, composites and templates are zero magnitude or brighter at 12 μm. These have been included for convenience and completeness in the AFBSC Version 1 in their original published forms.

Details concerning the catalog and its production are given in *An Explanatory Supplement to the Air Force Bright Spectral Catalog, Version 1.0* that is included in Appendix C. As has been mentioned previously, the AFBSC is an on-going program, and as such will occupy a major part of our effort during the next year.

5. ASTCAT VERSION 2.0

ASTCAT Version 2.0 is a set of 306 data files containing the times and coordinates at which moving solar system objects were scanned by MSX during the following data collection events (DCEs): CB01, CB02, CB03, CB04, CB05, CB06, CB09, and DC34. The files also contain an identification of the object scanned, a common name for the object, and an estimate of the irradiance in the SPIRIT III radiometer bands. The files are intended to be used to associate MSX point source detections with possible measurements of asteroids, planets, and comets. The database we used included the orbital elements of 12656 numbered asteroids, 17560 unnumbered asteroids, 173 comets, and 7 planets.

The algorithms and software implementation have been documented previously as an add-on to the PL DAC pipeline processor called ASTID (Walker and Schlapfer, 1994). The only difference from that software was the requirement to make the present software a stand-alone version producing association files that could be used in an off-line mode. This was successfully done for ASTCAT Version 1. ASTCAT Version 2.0 benefits from a fourfold increase in the number of asteroid orbital elements available in March of this year, as well as improved MSX definitive attitude files that are now available. The output format has been modified to include common names for all the objects scanned, thereby facilitating recognition of interesting objects.

This work is considered complete and no additional work will be undertaken during the coming year. Although we have had no feedback on the success of ASTCAT Version 2, it would be seem that an MSX catalog of small solar system bodies detected would be of benefit to the scientific community.

6. FUTURE PLANS

6.1 AFBSC

In the coming year we will work toward two further releases of the AFBSC, Versions 1.1 and 2.0.

AFBSC Version 1.1 – This release will be an extension of AFBSC 1.0 with the addition of those sources MSX observed but were not included in release 1.0. We have already extracted those MSX point sources brighter than zero mag. in bands A, B1, B2, C, D or E, and have merged the lists of sources. However, this resulted in on the order of 6000 objects, of which about 4000 are Band-E only sources. We believe that it is prudent to reject such objects and work with the 1701 sources above the zero magnitude threshold in at least 2 MSX bands, so as not to overwhelm the catalog by long-wavelength-only or very red sources.

The 1701 MSX sources have been compared with our basic list of 1638 IRAS sources and 804 matches were found, leaving 834 MSX sources to be considered further. The 1701 have also been searched for in the IRAS PSC2 and 1523 were found associated within a radius of 30 arcsec. We have not yet searched the IRAS Low Resolution Spectra (LRS) database for these sources. However, we anticipate that many will have useful spectra, since 1128 are among the original 2503 bright sources classified for the CBSD. Our main concern is confusion due to the large beam of the LRS and the high density of sources in the plane.

Adding the MSX sources can be expected to increase the number in the catalog to about 1900 sources. We target a release date for AFBSC Version 1.1 to about the middle of September 2000.

AFBSC Version 2.0 - In this version the spliced LRS and SKY 4 spectra will be normalized to all the well characterized photometry available. This will give us a basis to better quantify the effects of variability on the irradiance from these sources (at least in the case where the shape of the star's spectrum is not variable). Thus our major effort will be to

calibrate as much of the CIO photometry as possible. We will, at the same time, gather what information is available as to the phase of the photometric observations.

We will also include many of the "problem" sources that we previously culled from Versions 1.0 and 1.1. Many of these sources could not be represented by any spectrum in the SKY4 library. We will create a new grid of model AGB spectra using the DUSTY code (Ivezic, et al., 1999) to provide a wider range of spectrum selection. We believe that this could increase the total number of AFBSC sources to a number greater than 2000. Our target for release of the AFBSC Version 2.0 is February 2001.

6.2 SKY5

We propose to develop a 5th version of the SKY model of the point source sky for release to AFRL under our current PRDA contract. The goal is to secure a version optimized for operation in the range 2-35 μm. Upgrades to SKY4 embodied in SKY5 will include the following: a new extinction law; a more modern set of absolute magnitudes M_V; new space densities; a set of hardwired M_J and M_K that are self-consistent with the current spectral library supporting the SKY code (through which it achieves its flexibility to handle arbitrary user-supplied passbands). In all other respects, SKY5 will behave as SKY4 and its code will be very similar. It will be tested against a variety of new deep star counts spanning the range from V through MSX Band-E to assure the adequacy of its performance and intended improvements over SKY4.

We plan on two deliverables: the new code (LUM50 and all supporting programs and data files), and an explanatory document on the mechanics of using SKY5. We anticipate completing SKY5 by the end of January, 2001.

6.3 Zodiacal Data Processing

During the next year we will work on removing non-rejected Earth radiance (NRER) from MSX CB01 scans of the zodiacal dust near the Sun. Using Diffuse Background Files (DBF)

generated at the PL DAC we will apply our model of the SPIRIT III NRER, remove the side-lobe response to the Earth, and create a new set of DBFs cleaned of this sensor artifact to be returned to AFRL. The output file format will be the same as the DBF supplied. We will also document what was done and the model used. If time permits, we will create an ecliptic map of the zodiacal radiance seen by the CB01's.

We will also extract zodiacal radiance data from the Lunar OAR experiment DC32. The basic products will be files of radiance produced by co-adding the pixels along each scan as a function of time and ecliptic coordinate for each band. The final files will be at the maximum spatial resolution consistent with good SNR. We will attempt to remove the off axis radiance due to the Moon as appropriate. If time permits we will produce maps of the coadded scans and look for fine structures in the dust radiance. All procedures and models used will be fully documented.

REFERENCES

M. Cohen, R. G. Walker, M. J. Barlow, & J. R. Deacon 1992a, "I. Ground-Based and IRAS Broadband Calibrations," *Astron. J.*, **104**, 1650

M. Cohen, R. G. Walker, & F. C. Witteborn 1992b, "II. alpha Tau and the Recalibration of the IRAS Low Resolution Spectrometer," *Astron. J.*, **104**, 2030

M. Cohen, F. C. Witteborn, D. F. Carbon, G. C. Augason, D. Wooden, J. Bregman, & D. Goorvitch 1992c, "III. The Influence of CO and SiO," *Astron. J.*, **104**, 2045

M. Cohen, F. C. Witteborn, R. G. Walker, J. D. Bregman, & D. Wooden 1995, "IV. 1.2-35 micron Spectra of Six Standard Stars," *Astron. J.*, **110**, 275

M. Cohen & J. K. Davies 1995, "V. The Role of UKIRT and the CGS3 Spectrometer," *Mon. Notices of the Royal Astron.Soc*, **276**, 715

M. Cohen, F. C. Witteborn, J. D. Bregman, D. Wooden, A. Salama, & L. Metcalfe 1996, "VI. 3--35 micron Spectra of Three Southern Standard Stars," *Astron. J.*, **112**, 241

M. Cohen, F. C. Witteborn, D. F. Carbon, J. K. Davies, D. H. Wooden, & J. D. Bregman, 1996, "VII. New Composite Spectra, Comparison with Model Atmospheres, and Far--Infrared Extrapolations," *Astron. J.*, **112**, 2274

M. Cohen, F.C. Witteborn, T. Roush, J. Bregman, & D. Wooden 1998, "VIII. 5-14 micron Spectroscopy of the Asteroids Ceres, Vesta, & Pallas," *Astron. J.*, **115**, 1671

M. Cohen 1998, "IX. Calibrated Stellar Spectra using DIRBE Radiometry," *Astron. J.*, **115**, 2092

M. Cohen, R.G. Walker, B. Carter, P.L. Hammersley, M.R. Kidger, & K. Noguchi, K. 1999, "X. A Self-Consistent Radiometric All-Sky Network of Absolutely Calibrated Stellar Spectra," *Astron. J.*, **117**, 1864

Walker, R.G. and Schlapfer, M.F., 1994. "ASTID – Software Description," delivered to the PL DAC February 28, 1994

Ivezic, Z., Nenkova, M., and Elitzer, M., 1999, "User Manual for DUSTY," University of Kentucky Internal Report, accessible at http://www.pa.uky.edu/~moshe/dusty

Appendix A.

Spectral Irradiance Calibration in the Infrared. XII. Radiometric Measurements from the Midcourse Space Experiment (MSX)

Martin Cohen, Russell G. Walker, Sumita Jayaraman, Elizabeth Barker

Vanguard Research, Inc., Suite 204, 5321 Scotts Valley Drive, Scotts Valley, CA 95066

Electronic mail: mcohen@astro.berkeley.edu, (russ,sumita,ebarker)@vrisv.com

Stephan D. Price

Air Force Research Laboratory/VSBC, 29 Randolph Rd., Hanscom AFB, MA 01731

Electronic mail: Steve.Price@hanscom.af.mil

ABSTRACT

We describe the series of absolute stellar irradiance calibration experiments conducted by the Midcourse Space Experiment (MSX). These experiments validate the published absolute irradiances of our primary and secondary standards, namely α CMa and a set of bright K-M giant stars, and confirm their radiometric "closure" (relative irradiances). We also validate the absolute spectra of 28 of the fainter calibrators that have been previously published and create additional faint reference stars from the MSX data. This work underpins the absolute calibrators provided for DIRBE, IRTS, ISO, our all-sky network of 422 fainter calibration stars (Cohen et al. 1999: Paper X), the MSX Point Source Catalog, and is now being extended to accommodate calibrators for SIRTF.

Subject headings: infrared: stars — methods: analytical — techniques: spectroscopic – stars: late type – astronomical databases: miscellaneous

1. INTRODUCTION

The Midcourse Space Experiment (MSX) was initiated by the Strategic Defense Organization and flown by its successor entity, the Ballistic Missile Defense Organization. Mill et al. (1994) describes the MSX mission and the responsibilities of the eight PI teams. The infrared instrument on MSX, the SPatial InfraRed Imaging Telescope, or SPIRIT III, had two telemetry rates with several gain states in each to accommodate the widely diverse experimental objectives and the large range of backgrounds, from the hard Earth to space, that a given MSX observation, called a Data Collection Event or DCE, might encounter. An internal scan mirror was used with the high telemetry rate to rapidly sweep the five line-scanned focal plane arrays over $0.5° \times 1°$ to $1.5° \times 1°$ fields of regard. Most of the on-orbit calibration and instrument performance assessment observations were taken in the mirror-scan mode. All the astronomy experiments (Price et al. 1996) used the more sensitive mirror-fixed, low telemetry rate observing mode with spacecraft motion sweeping the line-scan arrays across the sky. The three lower gain, mirror-fixed modes, designated EL4, EL16 and EL16+, reduce the gain by nominal factor of four, 16 and 64, respectively. The 12-bit telemetry word has a dynamic range of ~4000 in the highest gain, and gain ranging gives a total dynamic range of $\sim 3 \times 10^5$. All the mirror-fixed gain states were used at one time or another to accommodate the very large dynamic range of the calibration standards adopted for the MSX Stellar Standards Experiment. To assure that all the experiments had the same calibration pedigree, MSX's Data Certification PI team coordinated the calibration of the instrument over its full range of operating parameters, that is, all gain states in both mirror-fixed and scanning mode, as a function of focal plane temperature. The Data Certification team conducted several hundred calibration and performance assessment measurements during the cryogen phase of the mission. Consequently, a large fraction, fully a quarter, of the DCEs obtained during the cryogen phase of the mission were devoted to the calibration and performance assessment of the

infrared instrument. Egan et al. (1999) provide more details on the SPIRIT III instrument and its ground-based and on-orbit calibration. In this paper we describe our efforts: (1) to validate, in space, the reference stellar spectra that support the absolute calibration of DIRBE, IRTS, and ISO through previously published absolute spectra for a number of different spectral types of calibrators; and (ii) to create several new, complete (1.2–35 μm), absolutely calibrated, "template" spectra.

The MSX astronomy experiments were designated CB-01 through CB-11 with the number reflecting the relative mission priority. We describe results from the CB-06 "Celestial Radiometric Standards" experiment in this article. Each CB-06 DCE obtained observations on a triad of stars, generally a fiducial reference star, flanked by two fainter stars that we wished to make into calibration sources. A DCE lasted about 30 min during which time we moved the spacecraft so that each star traversed the focal plane in a raster pattern of 0.75° amplitude, with small (200 μrad) cross-scan steps at each turnaround. Measurements of the dark currents of all focal plane pixels were made during every turnaround. Observations of a diffuse internal calibration stimulator were made at the beginning and end of each set of 20 raster legs. The pattern used for the 20 raster legs per star involved 10 scans, a cross-scan offset of about 0.5° and another 10 scans. This large offset was necessary to sample the two narrowband, short-wavelength arrays (so-called "B_1" and "B_2" bands) which each span only half the focal plane height, whereas the other four bands have full-height columns of $192 - 18.3''$ pixels. The structure of a triad means that we rely on the stability of the focal plane arrays for only about a 15-min period either to compare the irradiances of each fainter star with the bright reference star, or to assess absolute irradiances.

Table 1 lists the absolute attributes for zero magnitude for the six SPIRIT III infrared bands and relates lettered Band designations to their isophotal wavelengths for our standard

Kurucz model spectrum of Sirius (Cohen et al. 1992).

Table 2 lists the 24 CB-06 DCEs conducted during the cryogenic phase of the mission. Owing to the relative priority of the CB-06 experiment, many of the DCEs were obtained late in the mission. Unfortunately, the SPIRIT III focal plane warmed up toward the end of the cryogenic phase of the mission to the point where the temperatures exceeded the limit below which the ground-based and on-orbit absolute radiometric calibration and the attendant uncertainties were determined and considered valid. An assessment of data from all the astronomy experiments also indicates a marked decline in data quality the last week of cryolife, beginning at about CB0623. Thus, almost a third of the observations had to be rejected because the uncertainty assigned to the radiometry was too large to produce meaningful results. Fortunately, we were able to accomplish all of the major objectives of this experiment with the remaining DCEs.

2. DATA PROCESSING

The MSX program tasked the SPIRIT III sensor manufacturer, the Space Dynamics Laboratory of the Utah State University, to develop the data processing pipeline routine that corrects for instrumental effects on the data. This routine, designated standard CONVERT (we use the penultimate version - CONVERT 6.22), effectively linearizes the raw Level 1A telemetry data generating Level 2 data. The standard CONVERT routine subtracts the dark offset, corrects for the non-linear response of the detectors at large dynamic range values, flat-fields the data and corrects for trends in the array response as a function of focal plane temperature. The next step in the process is to apply an array response value to convert the data into Level 2A output as band-integrated calibrated radiance (units of W cm^{-2} sr^{-1}). The CONVERT processing has a final module, canonical CONVERT, that images the Level 2A data in focal plane coordinates and extracts point

sources from the result. Using this routine produced unacceptably large variations in photometry from scan leg to scan leg. Canonical CONVERT was originally coded for mirror-scan mode and subsequently modified for mirror-fixed data. It implicitly assumes a constant scan rate, a condition not met in the CB-06 DCEs.

Therefore, we extract the photometry of the star from images we create in celestial coordinates using Interactive Data Language (IDL) routines we developed specifically for that purpose. The Level 2A Extended Source Files are processed through POINTING_CONVERT 6.0, which assigns a position to each data value from the definitive attitude file created from the spacecraft attitude control and star-tracker information. The resulting Extended Source MAP file of time-tagged data values of radiance and celestial position for each leg of the raster scan is archived on tape. Each MAP file contained information on one star in one spectral band for one raster scan leg. The next step is to construct an image from each MAP file using an IDL routine we label CB06FINAL. CB06FINAL created an image of each scan in a $3° \times 3°$ window centered on the targeted star. The grid coordinates were Right Ascension and Declination, and the grid spacing was $9''$. The window was larger than the nominal $1° \times 0.75°$ scanned region to allow for an arbitrary scan angle, cross-scan steps, and the shift from observing the star in the upper third of the detector columns to the lower third.

Using the MAP file, a single (virtual) column image was created, and the noise, residual dark offset, and background radiance were measured for each pixel of the column. This was repeated for each column in the detector array for that band. A column image is simply the time history of the pixels' responses during the scan. The noise estimated here is essentially the sum of the dark noise, the photon noise from the mean background, and any noise due to radiance structure in the background. It does not include a significant amount of photon noise from bright sources. Dark offset and background radiance were not

separated, but were estimated as a total baseline offset. This was done by fitting a least squares first or second order polynomial to the pixel time history. The linear fit was used for observations taken in gain states EL16 and EL16+ used for the brightest stars where the bit size exceeded the rms noise of the sensor. Point sources and glitches were eliminated by rejecting outliers more than 2.5σ from the fit. Pixels with excessive noise were flagged and eliminated before image construction. The respective baselines were subtracted from the pixel outputs and the result weighted by the inverse variances and binned into the Right Ascension and Declination grid. Images of both the radiance and the standard deviation of the radiance were constructed. Sub-images $1.75° \times 1.75°$ centered on the target star were selected and written to FITS files.

The procedure PHOTOMETER_CB06 performed aperture photometry of the target stars. The FITS images from CB06FINAL were read by the procedure, cleaned of any single pixel events (spikes) that were present, and sub-arrays (101×101 pixels) centered on the star were selected for photometry of both source and background.

Aperture photometry was implemented using two techniques (Da Costa 1992; Stetson 1990): 1) the curve-of-growth method; and 2) the photometric profile method. The curve-of-growth method sums the radiance within a set of circular apertures of increasing radius centered on the star. If the baseline is truly zero, and in the absence of noise, the curve-of-growth will reach an asymptotic value when all the flux from the star has been included. The value of the asymptote can be taken as a measure of the brightness of the star. This method is useful for bright stars observed at a high signal-to-noise ratio (SNR). For faint stars the addition of the noise at large radii dominates the curve-of-growth process. The peak SNR for the stars we observed with SPIRIT III in CB-06 usually occurred at a radius of about 3 pixels from the star. The basis of the photometric profile method is that the shape of the curve-of-growth is determined only by the point response function

(PRF) of the telescope-detector system. Therefore, a measurement of the flux at optimum SNR can be corrected to the asymptotic value of the flux using the known curve-of-growth. Photometric profiles for each band were derived from observations of α Tau and α Boo, two of the three brightest stars in our set. In practice, the mean baseline of the sub-array is never exactly zero and an asymptote will never be reached. The curve-of-growth will continue to rise if the residual is positive, and will roll over and decrease if the residual is negative. To address this problem we iterated the mean baseline to bring the slope of the curve-of-growth to zero in the region 24 to 50 pixels (216″ to 450″) from the star. Two to three iterations were usually sufficient for convergence to within a small fraction of the noise.

The cleaned 101×101 pixel sub-arrays (0.25° × 0.25°) for flux and noise were saved as FITS images to be used for later coaddition. Pertinent information, such as scan number, name of flux and noise files used, median noise, residual background, source coordinates, irradiance of the target star determined from the curve-of-growth, the complete curve-of-growth, and the irradiance from the photometric profile method, were written to a photometry file.

The sub-arrays were then coadded using an interactive program, which displayed the entire set of both flux and noise images of each scan leg. Both mean and standard deviation images are produced in the coadd process and archived in FITS format. Aperture photometry was then performed on the target star in the coadded image using the same methods as used on the single scan images. The photometry from the coadded images is our principal result, with the photometry of the single scans providing a valuable check on the entire process.

Figure 1 illustrates a set of these coadded images for α Lyr, in all six radiometer bands. We chose this star because it is not particularly bright at the longer wavelengths

and, therefore, gives a fair representation of the noise associated with the coadded frames.

We were able to reconcile the irradiance values from the coadded images with the formal averages of the irradiances values from the images of the individual raster legs, after removing statistical outliers due to poor, noisy images by applying the theory of ordered statistics (Blom 1958; Mandel 1964). The irradiances calculated from the coadded images are the fundamental quantities that we have used in both the absolute and relative calibration experiments analyzed below.

3. ABSOLUTE IRRADIANCES OF THE SET OF COMPOSITES

Of primary importance was the direct comparison between measured and predicted absolute irradiances for those "composites" observed by MSX. The term "composite" denotes a star whose 1.2–35 μm spectrum has been fully observed in distinct segments and those segments have been assembled into a complete, continuous composite spectrum (Cohen, Walker & Witteborn 1992: CWW). Composites constitute the secondary reference stars in our scheme, being derived from our primary, α CMa. In this section we analyze the ratios of observed irradiances to those expected by integration of the SPIRIT III relative response curves over our published absolute stellar spectra. These ratios are available for a total of 23 to 26 measurements in each of the 6 bands based on the set of stars: α Boo, α CMa, α Lyr, α Tau, β And, β Gem, β Peg, γ Cru, and γ Dra. Table 3 presents these ratios for all combinations of DCE, star, and band.

If one isolates a single star, e.g. α Boo, then one finds irradiance values assessed from all the measurements within CB-06 with a spread, defined as (maximum-minimum)/average, of about 8–10 percent even in Band-A, the most sensitive band. Within a single DCE, the typical spread of irradiance values for one of the composites in Band-A, -C, and -D is about

10–20 percent, rising in Band-B_1, -B_2, and -E to 25–50 percent. Tables 4–9 summarize these spreads over the entire experiment, broken out by band, based on the ensemble of observed mean values for all DCEs on a given star, together with the average ratios of (observed/expected) irradiance for each star separately. All ensemble averages are formed by inverse variance weighting of the individual results.

Table 10 summarizes the well-determined average ratios of the irradiances for all the 6 bands, combining all the results from the ensemble of 9 bright reference stars to assess the absolute calibration in each band. We find excellent accord between measurement and expectation, thereby validating the absolute radiometric accuracy of this set of 9 fiduciary stellar spectra as follows: insignificantly different from expectation for Band-A (0.2±0.3 percent) and -C(0.9±0.5 percent); within 2.2±0.7 percent in -D, 2.6±0.8 percent in -B_1, 3.4±0.7 percent in -B_2, and 8.1±1.9 percent in -E (not in Table 10: see below). The value for Band-E may be biased upward by the inclusion of Vega's irradiance ratios because the known cool dust emission in this star is apparent longward of about 17 μm. Eliminating Vega, in Band-E only, leads to a weighted mean ratio for Band-E of (observed/expected)=1.075±0.019, or 7.5±1.9 percent, 4σ different from unity. Only in Band-E does Vega give an irradiance ratio statistically significant from 1, in accord with what is known already of the character of Vega's cool dust excess.

4. "CLOSURE" OF THE SET OF COMPOSITES

Another way to analyze CB-06 is by seeking "closure" among the set of 9 stars expressed in terms of the relative irradiances of one star to another. The first two DCEs of CB-06 involved triads consisting entirely of bright secondary standards. Analysis of these enables us to investigate the *relative* photometry of the composites observed. We have been able to compare γ Cru, β Peg, γ Dra, and α Lyr with α Boo, by comparing the differences in magnitudes observed with the differences in magnitudes that we expected.

For this ensemble of 5 stars we find closure in that the inverse-variance weighted average discrepancy in magnitude differences is insignificantly different from zero for all bands. Table 11 presents these results for individual stellar pairs, while Table 12 summarizes the results derived from this ensemble of all pairs (with respect to α Boo) on the relative closure of this subset of 5 stars.

Note that there are appreciable uncertainties in the *predicted* magnitude differences in Band-B_1 and -B_2 (Table 11). These arise because the in-band regions of these extremely narrow filters were designed to probe the very strong, terrestrial CO_2 absorption. Even from the altitudes attained by the Kuiper Airborne Observatory (KAO), these spectral regions were usually opaque. Consequently, there are portions of our empirical (composite) spectra of the bright K- and M-giants that could never be observed through the saturated CO_2 bands, and neighboring regions in which KAO spectra were obtained, but to which we conservatively assigned large uncertainties (10 percent: see CWW). These difficulties, coupled with the intrinsic steep decline of these cool stellar spectra into the CO fundamental band near 4.7 μm, result in sizeable uncertainties in predicted irradiance in Band-B_1 and -B_2. These uncertainties in no way reflect on the capabilities of SPIRIT III but, rather, represent empirical constraints in our composite spectra.

To provide a more stringent test of MSX data in these bands requires reliance on models, rather than empirical spectra, of hotter stars (types A-F), in which no such molecular features occur. Indeed, the predicted uncertainties in B_1- and B_2-magnitudes for our Kurucz Vega and Sirius models are only 0.020^m, quite indistinguishable from the uncertainties in Band-A, -C, -D, -E. Consequently, in their independent examination of the accuracy of the MSX Point Source Catalogs (version 1.2: Egan et al. 1999), Cohen, Hammersley & Egan (2000) investigate the photometry of stars over a wide range of spectral types in order to assess performance in Band-B_1 and -B_2, rather than relying solely

on composites and templates. Nonetheless, as Table 12 indicates, we have been able to validate the magnitude differences among 5 fiducial stars using CB-06, even in Band-B_1 and -B_2, albeit at the level of $\sim 0.05^m$.

We included some stars multiple times within CB-06, deliberately replicating DCEs on different dates to study the long-term reproducibility of SPIRIT III measurements. However, high noise afflicted several of these repeated measurements. We can say only that three twice-detected stars replicate their Band-A magnitudes within 0.026^m (τ^2 Ari), 0.044^m (31 Ori), and 0.057^m (δ Lep).

5. VALIDATING AND CREATING TEMPLATES

Of the 37 fainter stars that were observed in CB-06, seven were lost due to the poor performance near the end of cryolife. Two of the stars that were measured in CB-06, HD 91504=SAO222136 and HD 64144=26 Lyn, are actually of type K4III and, as such, are not formally templatable yet (i.e. we have never been able to assemble a complete, purely empirical, 1-35 μm spectrum for any exemplar of this type). The remaining 28 objects were among the 422 templates published in Paper X but, of these, seven were published solely on the basis of IRAS photometry, and another 16 were anchored only by IRAS and CalTech Two Micron Sky Survey (TMSS) K data. The relatively large uncertainties of their IRAS and TMSS photometry militate against well-determined scale factors. Thus, we could potentially validate and improve upon the quality (i.e. reduce the bias) of all 28 previously calibrated templates, substantially so in the case of 23.

In order to validate published templates, we will use solely CB-06 photometry to recreate templates for these same stars, and compare the space-based scale factors and biases with those published in 1999. Table 13 presents all usable radiometry from this

experiment on the fainter calibrators, in the form of magnitudes in the SPIRIT III bands (cf. Table 1).

Table 14 lists the HD numbers of all stars templated in this paper with links (in the electronic version) directly to the actual calibrated spectra, along with their radiometrically determined angular diameters (cf. Paper X). Table 14 offers the new multipliers and uncertainties (in the third and fourth columns, respectively) derived by templating the 28 stars solely using measurements in Table 13 and compares these values with those previously obtained using combined ground- and space-based (IRAS and/or DIRBE) photometry (in the fifth and sixth columns). We define template "validation" to mean that the multiplier±uncertainty values, determined from MSX radiometry alone, and those published in Paper X, using all photometry available at that time, overlap. For 27 of the 28 stars in Table 14 we can say that these overlaps are at less than the 1σ level. For one star, 45 Eri, the mean scales overlap at the 1.4σ level, perhaps as a consequence of the scattered provenance of this star's 4 usable measurements over 3 separate DCEs. Nonetheless, all 28 published templates are well-validated by MSX-only data drawn from CB-06. Consequently, the seventh and eighth columns of Table 14 give the new scale factors and reduced errors that result from refitting each stellar template to all the photometry available, including the MSX CB-06 measurements.

Thus, Table 14 implies that, for 28 stars, we have validated previous (Release 2.1: Paper X) absolutely calibrated templates and have generated new (Release 2.2: the current paper) absolute spectra with improved template biases (i.e. reduced uncertainties in reddened template multipliers) for all these stars compared with our earlier products.

Figure 2 illustrates 8 of these Release 2.2 templates, presenting all the supporting photometry used to normalize the reddened templates. Note the excellent accord between the SiO fundamental (near 8.2 μm) in these templates and the precision radiometry in

Band-A.

6. A GLOBAL PERSPECTIVE ON SPIRIT III MEASUREMENTS THROUGH CB-06

The CB-06 DCEs sample the entire cryogenic phase of the MSX mission, from 10 days after the initial performance and validation commissioning of the spacecraft to the last day of cryogen. Therefore, it is important to attempt to determine if any long-term trends are present in the CB-06 results arising from the secular increase in focal plane temperature. Complicating the issue is that shorter term focal plane temperature changes are imposed on this long-term trend, the amplitude of which depended on the length of time that a DCE preceding a CB-06 observation looked at the hard Earth. Schick and Bell (1997) speculated on the reasons why the SPIRIT III instrument was more susceptible to thermal pulses and why the focal plane temperatures were higher and rose faster than predicted. The focal plane temperature monitors indicate that the temperatures for the CB-06 DCEs increased in a fairly monotonic fashion throughout the mission. The Band-B focal plane temperature monitor indicated that the focal plane temperatures during the CB-06 DCEs increased fairly monotonically throughout the mission, rising from 11.2K for the first CB-06 DCE to 13.5K for the last event obtained 9.5 months later. The Band-B temperature monitor was found to be both more accurate and precise than those on the other focal plane modules.

We have been unable to discover any patterns linking the accuracy of CB-06 measurements with focal plane temperatures or mission time. For example, working from our published faint spectral templates, we have calculated the differences between expected magnitudes and those actually observed for the faint stars within the triads of CB-06. These differences show no trends with time or temperature. However, if we assess the performance throughout CB-06 by the mean difference for any band, using inverse-variance weighting, we find no statistically significant offsets for any band. These mean magnitude differences,

(observed-calculated), are: -.005±0.002 (Band-A), -.005±0.073 (-B1), -.033±0.022 (-B2), +0.036±0.012 (-C), +0.007±0.013 (-D), and +0.004±0.033 (-E).

Overall, we find very satisfactory accord between observation and expectation, in all six radiometers, and this is as true for the brightest as for the faintest stars studied in this experiment.

7. CONCLUSIONS

If we compare the observed irradiances with those predicted pre-launch from our published model, composite, and template stellar spectra, in each of the six bands, there are clear relationships with slopes essentially unity and offsets essentially zero. Table 15 presents these parameters, defined by least-squares fitting in linear-linear space, using the absolute irradiances and their uncertainties appropriately. Note that Figures 3-8 are presented in log-log space because the many faint stars would not otherwise be distinguishable as the bright fiducial stars dominate most of the dynamic range plotted. All stars measured from DCEs CB0604 through CB0626 were used to define these trends, and each is plotted with error bars corresponding to its 1σ absolute uncertainties. The fact that we have been able to validate the previously published (Paper X) faint stellar templates, by means of SPIRIT III, justifies our inclusion of their predicted irradiances in this analysis.

Using solely the absolute radiometry from one particular experiment on MSX we have achieved the following:

1) absolute validation of our published calibrated spectra of 9 bright reference stars to < 1 percent (Band-A,-C), ~ 2 percent (-D), ~ 3 percent (-B_1,-B_2), and 7-8 percent (-E);

2) validation of the relative calibration of 5 stellar composites or models: γ Cru, β Peg, γ Dra, α Lyr, and α Boo;

3) validation of 23 previously released calibrated stellar templates;

4) the creation of 28 new, improved calibrated templates, available by links in the electronic version of this paper.

The primary consequence of these absolute validations is that these same stellar spectra furnished absolute references for the calibration of DIRBE (Bands 1-5), the Near- and Mid-Infrared Spectrometers on the Infrared Telescope in Space, ESA's Infrared Space Observatory, as well as MSX's Point Source Catalogs and its Atlas of the Galactic Plane (images). Our framework unites spectroscopy and photometry in a self-consistent fashion and will embrace the calibrators for SIRTF's instruments in future papers of this series.

This work was supported under contract F19628-98-C-0047 with VRI by the Air Force Research Laboratory, who also provided the Level 1A raw data tapes for the CB-06 experiment. We are grateful for the loan of an SGI Indigo computer by Alan Thurgood of the Space Dynamics Laboratory, Utah State University.

REFERENCES

Blom, G. 1958, Statistical Estimates and Transformed Beta-Variables, John Wiley & Sons, New York

Cohen, M., Hammersley, P. L., & Egan, M. P. 2000, Radiometric validation of the Midcourse Space Experiment's (MSX) Point Source Catalogs & the MSX properties of normal stars, *Astron.J.*, **120**, 3362

Cohen, M., Walker, R. G., Barlow, M. J. & Deacon, J. R. 1992, Spectral Irradiance Calibration in Spectral Irradiance Calibration in the Infrared. I. Ground-Based and IRAS Broadband Calibrations, *Astron.J.*, **104**, 1650

Cohen, M., Walker, R.G., Carter, B., Hammersley, P., Kidger, M., & Noguchi, K., 1999, Spectral Irradiance Calibration in the Infrared. X. A Self-Consistent Radiometric All-Sky Network of Absolutely Calibrated Stellar Spectra, *Astron.J.*, **117**, 1864 (Paper X)

Cohen, M., Walker, R. G., & Witteborn, F. C. 1992b, Spectral Irradiance Calibration in the Infrared. II. Alpha Tau and the Recalibration of the IRAS Low Resolution Spectrometer, *Astron.J.*, **104**, 2030 (CWW)

Da Costa, G.S. 1992, in Astronomical CCD Observing and Reduction Techniques, ASP Conference Series, Vol. 23 (ed. S.B. Howell)

Egan, M.P. et al. 1999, "The *Midcourse Space Experiment* Point Source Catalog Version 1.2 Explanatory Guide", Air Force Research Laboratory Technical Report, AFRL-VS-TR 1999-1522, ADA 381933

Mandel, J. 1964, The Statistical Analysis of Experimental Data, John Wiley & Sons, New York

Mill, J., O'Neil, R. R., Price, S. D., Romick, G. J., Uy, O. M., & Gaposchkin, E. M. 1994, Midcourse Space Experiment: Introduction to the Spacecraft, Instruments and Scientific Objectives, *AIAA*, **31**, 900

Price, S.D. et al. 1996, Astronomy of the Midcourse Space Experiment, Proc. IAU Symp. 179, eds. B. J. McLean, D. A. Golombek, J. E. Hayes, H. E. Payne (Kluwer Academic), p.115

Schick, A. & Bell, G. 1997, Performance of the SPIRIT III cryogenic system, SPIE, 3122, 69

Stetson, P.B. 1990, On the growth-curve method for calibrating stellar photometry with CCDs , *Publ. Astron. Soc. Pacific*, **102**, 932

Table A-1: Zero Magnitude Attributes of SPIRIT III Bands

Filter	Bandwidth μm Uncertainty μm	In-Band W cm^{-2} Uncertainty W cm^{-2}	$F_{\lambda(iso)}$ W cm^{-2} μm^{-1} Uncertainty W cm^{-2} μm^{-1}	λ(iso) μm Uncertainty μm	Bandwidth Hz Uncertainty Hz	$F_{\nu(iso)}$ Jy Uncertainty Jy	ν(iso) Hz Uncertainty Hz
B_1	0.1036	3.279E-16	3.165E-15	4.294	1.685E+12	194.59	6.979E+13
	0.0012	6.075E-18	5.094E-17	0.0177	1.917E+10	3.134	5.818E+11
B_2	0.1794	5.364E-16	2.989E-15	4.356	2.840E+12	188.84	6.875E+13
	0.0018	9.415E-18	4.129E-17	0.0153	2.775E+10	2.606	4.866E+11
A	3.3620	8.196E-16	2.438E-16	8.276	1.402E+13	58.485	3.715E+13
	0.0124	1.225E-17	1.189E-18	0.0103	4.632E+10	0.269	8.840E+10
C	1.7205	9.259E-17	5.382E-17	12.126	3.493E+12	26.506	2.477E+13
	0.0267	1.917E-18	1.150E-18	0.0642	5.239E+10	0.556	2.593E+11
D	2.2344	5.686E-17	2.545E-17	14.649	3.109E+12	18.288	2.050E+13
	0.0669	1.767E-18	1.034E-18	0.1490	8.887E+10	0.725	4.132E+11
E	6.2440	3.555E-17	5.694E-18	21.336	4.041E+12	8.799	1.418E+13
	0.3298	1.667E-18	3.935E-19	0.3705	1.942E+11	0.577	4.598E+11

Table A-2: Details of MSX's "CB-06" Experiment

DCE	Date/UT	Star-1	Star-2	Star-3
CB0604	96/06/21/04:14:36	γ Cru	α Boo	β Peg
CB0605	96/07/03/04:56:49	α Boo	γ Dra	α Lyr
CB0606	96/10/08/04:47:36	SAO248381	α Lyr	42 Dra
CB0607	96/10/14/03:48:02	IRC+50004	SAO783	β Gem
CB0608	96/12/31/06:14:44	α Ari	β And	4 UMi
CB0609	97/01/14/07:02:21	60 And	α Tau	16 Aur
CB0610	97/01/20/01:43:02	SAO195639	α CMa	45 Eri
CB0613	97/01/27/17:16:02	GL4509S	α CMa	π^6 Ori
CB0614	97/01/28/04:24:05	31 Ori	α Tau	40 Cam
CB0615	97/01/29/00:56:19	β Col	α Tau	ι Aur
CB0616	97/02/01/00:35:02	β Vol	α CMa	24 Per
CB0617	97/02/02/00:38:02	γ^2 Vol	α CMa	τ^2 Ari
CB0618	97/02/04/01:01:02	δ Lep	α CMa	31 Ori
CB0619	97/02/04/04:29:16	δ Lep	α CMa	45 Eri
CB0620	97/02/03/00:13:02	24 Com	α Boo	SAO250019
CB0621	97/02/08/01:01:47	SAO223297	α CMa	τ^2 Ari
CB0622	97/02/10/14:10:02	6 Dra	α Boo	SAO222136
CB0623	97/02/15/11:43:02	SAO249451	α CMa	56 Ori
CB0624	97/02/16/11:48:02	γ Pic	α CMa	45 Eri
CB0625	97/02/23/13:17:02	ρ Ser	α Boo	51 Hya
CB0626	97/02/24/13:20:02	ρ Ser	α Boo	51 Hya
CB0631	97/02/24/16:37:54	26 Lyn	α Boo	IRC+10266
CB0632	97/02/25/00:33:21	6 Pup	α CMa	18 Mon
CB0633	97/02/25/16:54:52	32 Com	αBoo	SAO250979

Table A-3: Absolute Irradiance Ratios, (observed/expected), for the Ensemble of Bright Fiduciary Stars

DCE#	Star	Band-B_1	Band-B_2	Band-A	Band-C	Band-D	Band-E
04	γ Cru	0.926±0.055	0.937±0.050	0.936±0.019	0.945±0.025	1.027±0.035	1.036±0.059
04	α Boo	1.017±0.064	0.987±0.054	1.002±0.018	0.948±0.022	1.033±0.035	1.003±0.050
04	β Peg	0.874±0.063	0.964±0.070	1.038±0.020	1.068±0.026	1.073±0.036	1.082±0.056
05	α Boo	1.006±0.067	0.971±0.054	0.999±0.019	0.937±0.022	1.023±0.034	0.992±0.048
05	γ Dra	1.139±0.156	1.011±0.111	0.975±0.011	0.985±0.019	1.008±0.033	1.035±0.060
05	α Lyr	0.985±0.049	1.032±0.055	1.026±0.017	1.000±0.040	1.095±0.050	1.048±0.149
06	α Lyr	1.017±0.064	1.034±0.058	1.020±0.016	1.064±0.032	1.044±0.052	1.306±0.110
07	β Gem	0.982±0.153	0.966±0.112	0.976±0.020	1.017±0.025	1.005±0.037	1.185±0.072
08	β And	0.937±0.042	0.938±0.026	0.964±0.017	1.027±0.022	1.001±0.033	0.972±0.059
09	α Tau	0.992±0.064	0.999±0.058	0.962±0.018	1.048±0.027	1.038±0.035	1.053±0.054
10	α CMa	1.112±0.024	1.020±0.039	1.019±0.017	1.068±0.026	1.037±0.034	1.072±0.136
13	α CMa	0.801±0.073	0.962±0.029	1.019±0.016	1.041±0.036	1.014±0.036	1.099±0.060
14	α Tau	1.083±0.068	0.971±0.054	0.976±0.017	1.040±0.025	1.023±0.035	1.064±0.053
15	α Tau	1.023±0.072	1.013±0.061	0.959±0.019	1.004±0.027	1.021±0.036	1.110±0.059
16	α CMa	1.054±0.025	1.029±0.057	1.026±0.017	0.992±0.025	1.015±0.043	1.112±0.066
17	α CMa	1.198±0.026	0.895±0.038	0.995±0.016	1.050±0.038	0.984±0.038	1.047±0.166
18	α CMa	0.980±0.025	0.924±0.020	1.022±0.015	0.965±0.021	1.030±0.042	1.201±0.178
19	α CMa	0.896±0.021	0.967±0.039	1.006±0.017	1.008±0.027	1.056±0.039	1.070±0.056
20	α Boo	1.052±0.067	0.979±0.051	0.978±0.018	0.988±0.025	1.013±0.036	1.051±0.056
21	α CMa	1.032±0.025	0.970±0.021	1.013±0.015	1.013±0.076	1.010±0.042	1.018±0.141
22	α Boo	0.983±0.064	0.988±0.054	0.985±0.020	0.990±0.022	1.014±0.035	1.125±0.063
23	α CMa	1.137±0.031	0.972±0.022	1.010±0.016	1.001±0.022	1.065±0.035	1.238±0.084
24	α CMa	0.946±0.089	0.982±0.020	1.004±0.017	0.975±0.044	0.971±0.031	1.155±0.093
25	α Boo			1.019±0.018	0.935±0.021	1.028±0.038	1.322±0.065
26	α Boo			0.999±0.020	0.885±0.026	1.013±0.043	
31	α Boo			1.014±0.017	0.943±0.029	1.000±0.033	

Table A-4: Spreads & Irradiance Ratios for Bright Reference Stars, in Band-B_1 After Rejection of Outliers

Star	#	spread(%)	weighted average	σ
α Boo	4	6.8	1.014	0.033
α CMa	9	39	1.039	0.009
α Lyr	2	3.2	0.997	0.039
α Tau	3	8.8	1.031	0.039
β And	1	21	0.937	0.042
β Gem	1	38	0.982	0.153
β Peg	1	7.0	0.874	0.063
γ Cru	1	13	0.926	0.055
γ Dra	1	39	1.139	0.156

Table A-5: Spreads & Irradiance Ratios for Bright Reference Stars, in Band-B_2 After Rejection of Outliers

Star	#	spread(%)	weighted average	σ
α Boo	7	1.7	1.000	0.007
α CMa	9	14	1.013	0.007
α Lyr	2	0.2	1.023	0.012
α Tau	3	4.2	0.966	0.010
β And	1	8.1	0.938	0.026
β Gem	1	22	0.966	0.112
β Peg	1	15	0.964	0.070
γ Cru	1	20	0.937	0.050
γ Dra	1	36	1.011	0.111

Table A-6: Spreads & Irradiance Ratios for Bright Reference Stars, in Band-A After Rejection of Outliers

Star	#	spread(%)	weighted average	σ
α Boo	7	4.1	1.000	0.007
α CMa	9	3.1	1.013	0.007
α Lyr	2	0.6	1.023	0.012
α Tau	3	1.8	0.966	0.010
β And	1	14	0.964	0.017
β Gem	1	10	0.976	0.020
β Peg	1	13	1.038	0.020
γ Cru	1	15	0.936	0.019
γ Dra	1	13	0.975	0.011

Table A-7: Spreads & Irradiance Ratios for Bright Reference Stars, in Band-C After Rejection of Outliers

Star	#	spread(%)	weighted average	σ
α Boo	7	11	0.948	0.009
α CMa	9	10	1.007	0.010
α Lyr	2	6.2	1.039	0.025
α Tau	3	4.3	1.031	0.015
β And	1	5.3	1.027	0.022
β Gem	1	26	1.017	0.025
β Peg	1	13	1.068	0.026
γ Cru	1	11	0.945	0.025
γ Dra	1	16	0.985	0.019

Table A-8: Spreads & Irradiance Ratios for Bright Reference Stars, in Band-D After Rejection of Outliers

Star	#	spread(%)	weighted average	σ
α Boo	7	3.2	1.017	0.014
α CMa	9	9.2	1.019	0.012
α Lyr	2	4.8	1.071	0.036
α Tau	3	1.7	1.027	0.020
β And	1	15	1.001	0.033
β Gem	1	22	1.005	0.037
β Peg	1	13	1.073	0.036
γ Cru	1	13	1.027	0.035
γ Dra	1	22	1.008	0.033

Table A-9: Spreads & Irradiance Ratios for Bright Reference Stars, in Band-E After Rejection of Outliers

Star	#	spread(%)	weighted average	σ
α Boo	5	30	1.074	0.025
α CMa	9	20	1.112	0.028
α Lyr	2	22	1.215	0.088
α Tau	3	5.3	1.074	0.032
β And	1	42	0.972	0.059
β Gem	1	44	1.185	0.072
β Peg	1	25	1.082	0.056
γ Cru	1	17	1.036	0.059
γ Dra	1	50	1.035	0.060

Table A-10: Closure of the Ensemble of 9 Fiduciary Calibrators

Band	#	weighted average	σ
B_1	23	1.026	0.009
B_2	23	0.966	0.007
A	26	0.998	0.003
C	26	0.991	0.005
D	26	1.022	0.008
E	24	1.075	0.019

Table A-11: Magnitude Differences Between Pairs of Fiduciary Stars

DCE	Star	Reference	Band	Observed Δmag	Predicted Δmag	Observed-Predicted
CB0604	γ Cru	α Boo	B_1	-0.054±0.020	-0.155±0.089	0.101±0.091
CB0604	γ Cru	α Boo	B_2	-0.100±0.029	-0.156±0.076	0.056±0.081
CB0604	γ Cru	α Boo	A	-0.201±0.012	-0.274±0.028	0.073±0.030
CB0604	γ Cru	α Boo	C	-0.265±0.013	-0.269±0.036	0.004±0.038
CB0604	γ Cru	α Boo	D	-0.266±0.013	-0.271±0.049	0.005±0.051
CB0604	γ Cru	α Boo	E	-0.294±0.016	-0.250±0.078	-0.044±0.080
CB0604	β Peg	α Boo	B_1	0.749±0.014	0.777±0.107	-0.028±0.108
CB0604	β Peg	α Boo	B_2	0.788±0.025	0.763±0.092	0.025±0.095
CB0604	β Peg	α Boo	A	0.685±0.012	0.723±0.027	-0.038±0.030
CB0604	β Peg	α Boo	C	0.564±0.014	0.692±0.034	-0.128±0.037
CB0604	β Peg	α Boo	D	0.628±0.012	0.670±0.049	-0.042±0.050
CB0604	β Peg	α Boo	E	0.600±0.022	0.683±0.072	-0.083±0.075
CB0605	γ Dra	α Boo	B_1	1.645±0.050	1.781±0.148	-0.136±0.156
CB0605	γ Dra	α Boo	B_2	1.730±0.047	1.773±0.119	-0.043±0.128
CB0605	γ Dra	α Boo	A	1.707±0.014	1.681±0.021	0.026±0.025
CB0605	γ Dra	α Boo	C	1.615±0.015	1.669±0.030	-0.054±0.034
CB0605	γ Dra	α Boo	D	1.684±0.017	1.667±0.047	0.017±0.050
CB0605	γ Dra	α Boo	E	1.639±0.041	1.686±0.070	-0.047±0.081
CB0605	α Lyr	α Boo	B_1	3.098±0.055	3.075±0.069	0.023±0.088
CB0605	α Lyr	α Boo	B_2	2.975±0.060	3.039±0.058	-0.064±0.083
CB0605	α Lyr	α Boo	A	3.099±0.014	3.129±0.025	-0.030±0.029
CB0605	α Lyr	α Boo	C	3.112±0.039	3.182±0.033	-0.070±0.051
CB0605	α Lyr	α Boo	D	3.102±0.037	3.175±0.048	-0.073±0.061
CB0605	α Lyr	α Boo	E	3.134±0.146	3.195±0.071	-0.061±0.162

Table A-12: Weighted Average (observed-predicted) Δmag for 4 Fiduciary Stars & α Boo

Band	<observed-predicted>	$\pm\sigma$
B_1	0.019	0.050
B_2	-0.001	0.046
A	0.009	0.014
C	-0.061	0.019
D	-0.019	0.026
E	-0.059	0.045

Table A-13: Usable Radiometry on Fainter Stars from CB-06 in Magnitudes; Repeated Star Names Denote Data from Different DCEs

Star (HD)	Name	[4.29]	[4.36]	[8.28]	[12.13]	[14.65]	[21.34]
1240	IRC+50004	...	1.484±0.095	1.513±0.008	1.366±0.038	1.586±0.051	...
8810	SAO248381	1.836±0.308	1.987±0.254	2.034±0.013	1.841±0.187	1.874±0.055	
12929	α Ari	...	-0.600±0.083	-0.790±0.012	-0.649±0.026	-0.638±0.050	-0.799±0.199
13520	60 And	...	1.235±0.092	1.177±0.009	1.184±0.046	1.319±0.149	1.202±0.340
18449	24 Per	...	...	2.184±0.011	1.985±0.191	2.288±0.267	...
20893	τ^2 Ari	...	...	2.163±0.019	...	...	...
20893	τ^2 Ari	...	...	2.189±0.013	...	...	...
28749	45 Eri	...	...	1.800±0.019	...	1.674±0.226	...
28749	45 Eri	...	1.789±0.255	...	...	...	...
28749	45 Eri	...	...	...	1.627±0.274	...	...
30338	SAO783	...	1.650±0.123	1.957±0.008	1.914±0.061	1.941±0.097	...
31398	ι Aur	-0.800±0.085	-0.664±0.054	-0.845±0.012	-0.862±0.018	-0.867±0.017	-0.875±0.035
31767	π^6 Ori	...	1.211±0.264	1.288±0.003	1.230±0.053	1.220±0.051	...
33872	SAO195639	...	...	2.249±0.036	2.257±0.079	1.937±0.176	...
34334	16 Aur	...	1.467±0.173	1.363±0.010	1.485±0.067	1.198±0.067	...
36167	31 Ori	...	0.925±0.057	0.711±0.013	0.753±0.138	0.783±0.081	...
36167	31 Ori	...	1.003±0.332	0.755±0.012	...	0.543±0.135	...
39364	δ Lep	...	1.025±0.125	1.274±0.012	1.139±0.106	1.017±0.200	1.057±0.259
39364	δ Lep	...	...	1.217±0.012	1.251±0.112	1.131±0.050	...
39400	56 Ori	...	...	1.605±0.021	1.129±0.123	1.401±0.112	...
39425	β Col	...	0.392±0.047	0.445±0.014	0.529±0.042	0.549±0.142	...
39523	γ Pic	...	...	1.947±0.006	...	1.622±0.212	...
42540	SAO249451	...	...	2.153±0.015	...	...	...
42633	40 Cam	...	2.077±0.133	2.411±0.080	...	...	...
46815	GL4509S	...	...	2.190±0.022	...	...	...
55865	γ^2 Vol	1.064±0.327	...	1.319±0.017	...	1.344±0.087	...
65662	SAO250019	...	...	2.085±0.011	...	...	...
71878	β Vol	...	...	1.150±0.008	1.009±0.239	1.412±0.191	...
91504	SAO222136	...	...	2.430±0.010	...	2.583±0.330	...
106321	SAO223297	...	...	1.805±0.005	1.781±0.291	...	...
109511	24 Com	...	...	2.361±0.010	2.141±0.211	...	...
109551	6 Dra	...	1.435±0.295	1.530±0.020	...	...	...
124547	4 UMi	...	1.247±0.279	1.439±0.005	...	...	...
141992	ρ Ser	...	...	...	0.979±0.106	...	...
141992	ρ Ser	...	...	1.011±0.008	...	0.563±0.213	...
170693	42 Dra	1.895±0.193	2.073±0.066	1.899±0.007	1.837±0.063	2.082±0.197	1.748±0.149

Table A-14: Validation of Existing Templates by CB-06 Data

Star (HD)	Name	CB-06 only		Published		New: all data		
		Scale	Error	Scale	Error	Scale	Error	Angular Diam. ±unc.(mas)
1240	IRC+50004	3.675E-2	1.063E-3	3.789E-2	3.931E-4	3.762E-2	3.680E-4	2.61±0.028
8810	SAO248381	1.034E-2	5.975E-4	9.725E-3	1.366E-4	9.768E-3	1.291E-4	2.07±0.025
12929	α Ari	1.117E-1	1.333E-3	1.105E-1	8.183E-4	1.103E-1	6.962E-4	6.89±0.073
13520	60 And	1.026E-1	1.177E-3	1.019E-1	2.648E-3	1.024E-1	1.071E-3	2.95±0.033
18449	24 Per	8.643E-3	2.265E-4	8.655E-3	2.061E-4	8.665E-3	2.031E-4	1.93±0.030
20893	τ^2 Ari	4.096E-2	1.183E-2	4.034E-2	9.721E-4	4.083E-2	4.328E-4	1.86±0.021
28749	45 Eri	5.820E-2	1.093E-3	5.430E-2	1.719E-3	5.705E-2	9.348E-4	2.20±0.028
30338	SAO783	4.852E-2	2.286E-3	5.020E-2	5.491E-4	4.988E-2	4.987E-4	2.06±0.023
31398	ι Aur	6.424E-1	1.683E-2	6.492E-1	6.927E-3	6.465E-1	6.366E-3	7.41±0.081
31767	π^6 Ori	1.729E-2	4.363E-4	1.715E-2	1.481E-4	1.716E-2	1.400E-4	2.72±0.030
33872	SAO195639	8.544E-3	1.842E-4	7.920E-3	2.470E-4	8.248E-3	1.439E-4	1.90±0.025
34334	16 Aur	8.487E-2	2.613E-3	8.663E-2	1.043E-3	8.623E-2	9.684E-4	2.70±0.030
36167	31 Ori	3.060E-2	7.609E-4	3.194E-2	3.109E-4	3.166E-2	2.860E-4	3.72±0.041
39364	δ Lep	1.080E-1	2.590E-3	1.050E-1	9.902E-4	1.051E-1	9.256E-4	2.60±0.028
39400	56 Ori	1.408E-2	4.331E-4	1.311E-2	2.672E-4	1.323E-2	2.218E-4	2.39±0.031
39425	β Col	3.698E-2	4.448E-4	3.700E-2	5.186E-4	3.612E-2	2.487E-4	3.95±0.042
39523	γ Pic	9.306E-3	4.415E-4	9.349E-3	9.420E-5	9.341E-3	8.688E-5	2.01±0.022
42540	SAO249451	4.506E-2	2.013E-3	4.196E-2	7.004E-4	4.324E-2	5.226E-4	1.92±0.022
42633	40 Cam	3.900E-2	1.050E-3	3.658E-2	2.421E-3	3.824E-2	9.529E-4	1.80±0.029
46815	GL4509S	8.225E-3	1.411E-4	4.277E-2	9.740E-4	4.129E-2	6.609E-4	1.87±0.024
55865	γ^2 Vol	9.734E-2	4.240E-3	9.735E-1	1.680E-3	9.737E-2	1.087E-3	2.50±0.029
65662	SAO250019	4.564E-3	2.268E-3	4.488E-2	5.961E-4	4.482E-2	5.388E-4	1.95±0.022
71878	β Vol	1.980E-2	9.040E-4	1.944E-2	2.177E-4	1.951E-2	1.905E-4	2.90±0.033
106321	SAO223297	5.686E-2	6.819E-4	5.795E-2	5.670E-4	5.708E-2	4.327E-4	2.20±0.023
109511	24 Com	6.383E-3	2.326E-4	6.385E-3	7.961E-5	6.385E-3	7.523E-5	1.66±0.019
109551	6 Dra	7.577E-3	1.802E-4	7.457E-2	1.510E-3	7.499E-2	1.145E-3	2.52±0.031
124547	4 UMi	8.074E-2	1.832E-3	8.104E-2	7.927E-4	8.096E-2	7.253E-4	2.62±0.028
141992	ρ Ser	2.639E-2	3.434E-4	2.500E-2	8.537E-4	2.533E-2	2.173E-4	3.33±0.036
170693	42 Dra	9.545E-3	1.952E-4	9.753E-4	9.975E-5	9.709E-3	8.929E-5	2.05±0.023

Table A-15: Least-Squares Fits Throughout CB-06 Between Observed and Predicted Irradiances

Parameter	4.29μm	4.36μm	8.28μm	12.13μm	14.65μm	21.34μm
Slope	1.035±0.006	1.028±0.024	1.039±0.007	1.026±0.010	0.973±0.004	0.947±0.010
Offset (E-17)	-2.8±2.9	-1.6±6.8	-2.0±2.3	-0.43±0.64	0.12±0.15	0.03±0.40
# stars	38	13	25	29	29	13

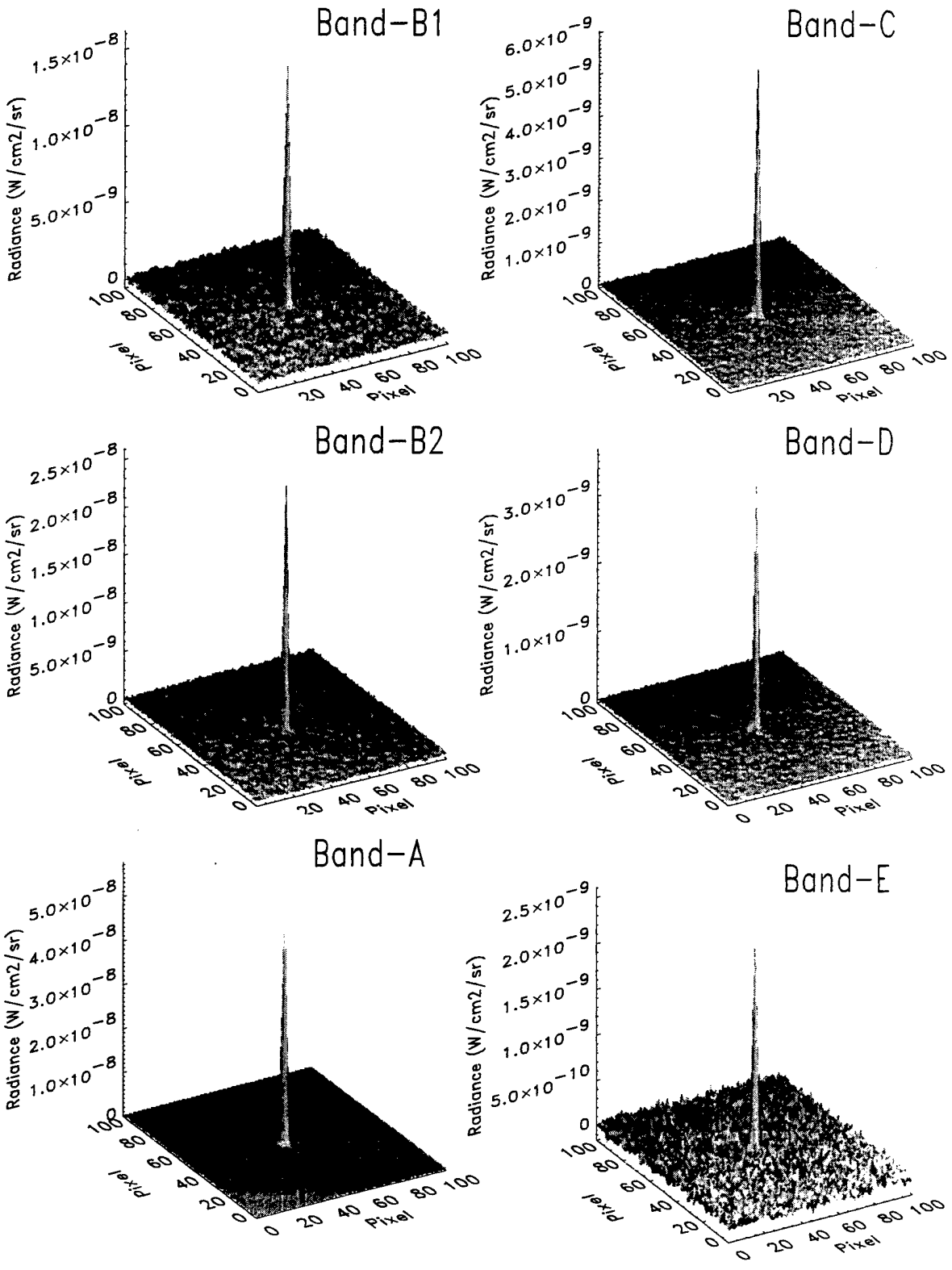

Figure-A1: The Coadded Images of α Lyr in Each of the 6 SPIRIT III Radiometers. Small Subimages containing 101×101 Pixels are Presented.

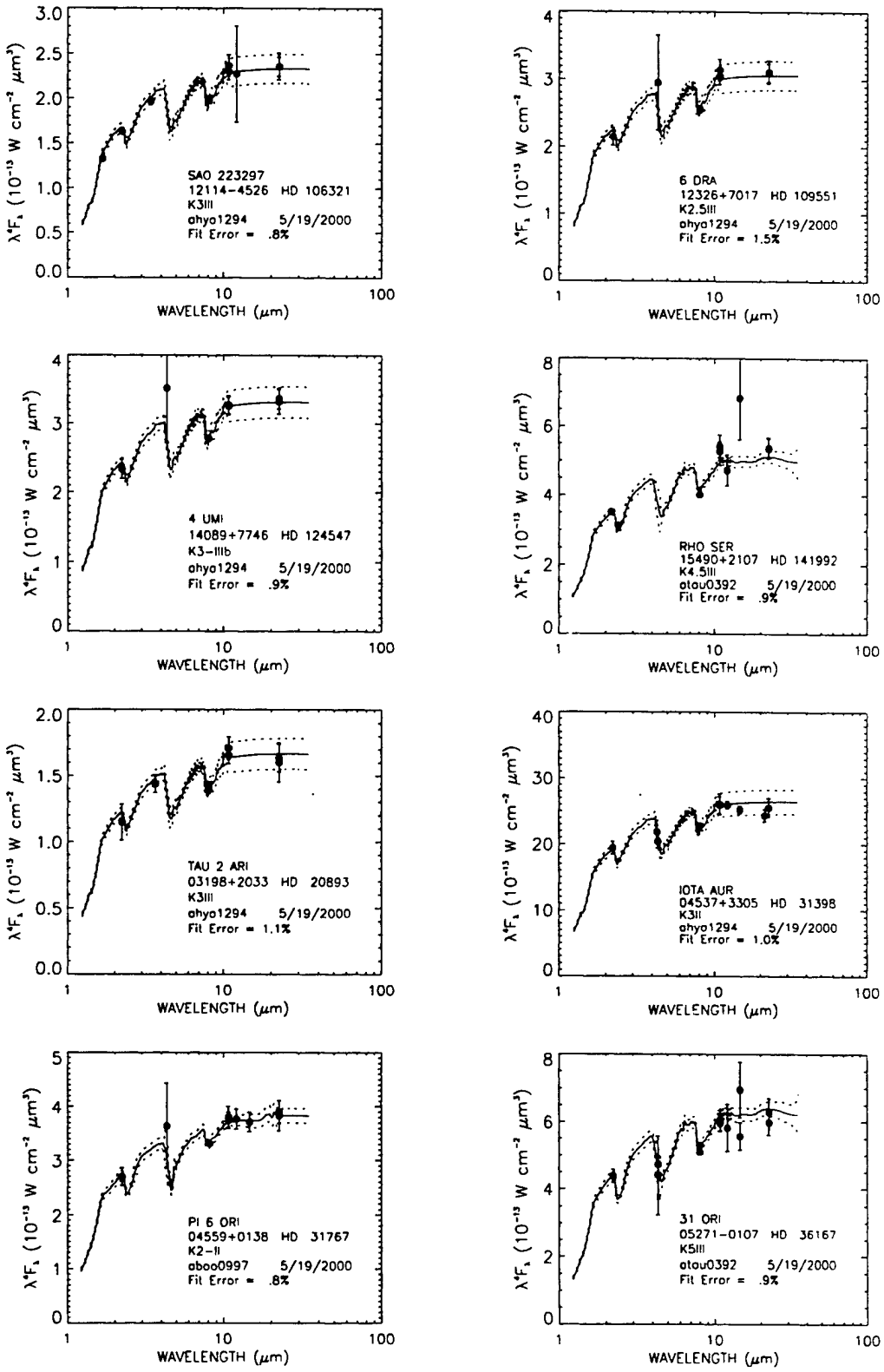

Figure A-2: Eight of the 28 Calibrated Stellar Templates Newly-Created in this Paper. Each plot shows, and documents, the normalized, reddened template and the photometry to which it was fitted.

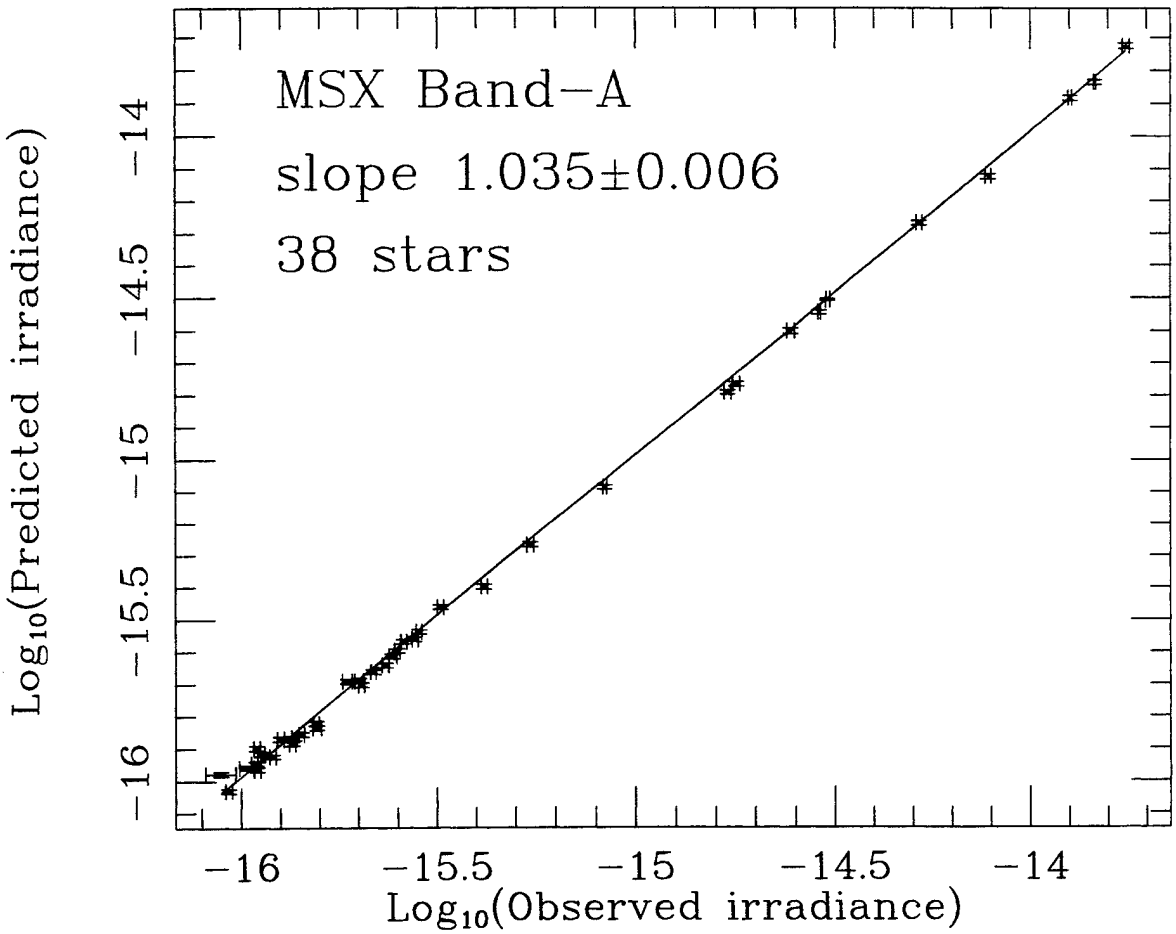

Figure A-3: The Relationship Between SPIRIT III's Observed Irradiance and our Pre-Launch Expectations for 38 Stars From CB-06 Measured in Band-A. The plot is in log-log space but the least-squares fits (Table 15) were derived from the linear trends. Best fit relationship is shown by the dashed curve. $\pm 1\sigma$ absolute error bars are shown.

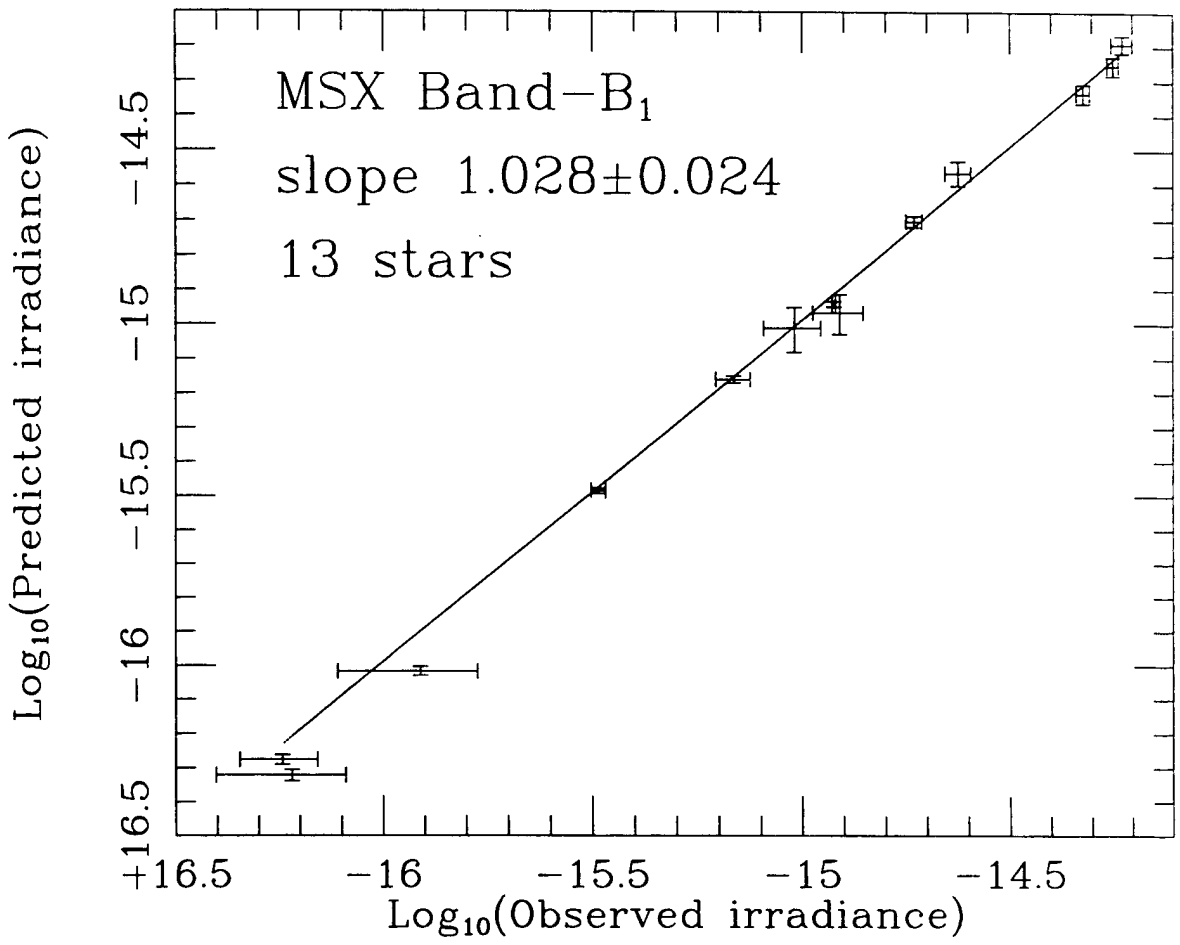

Figure A-4: As in Figure A-3 but for Band-B_1 Measurements.

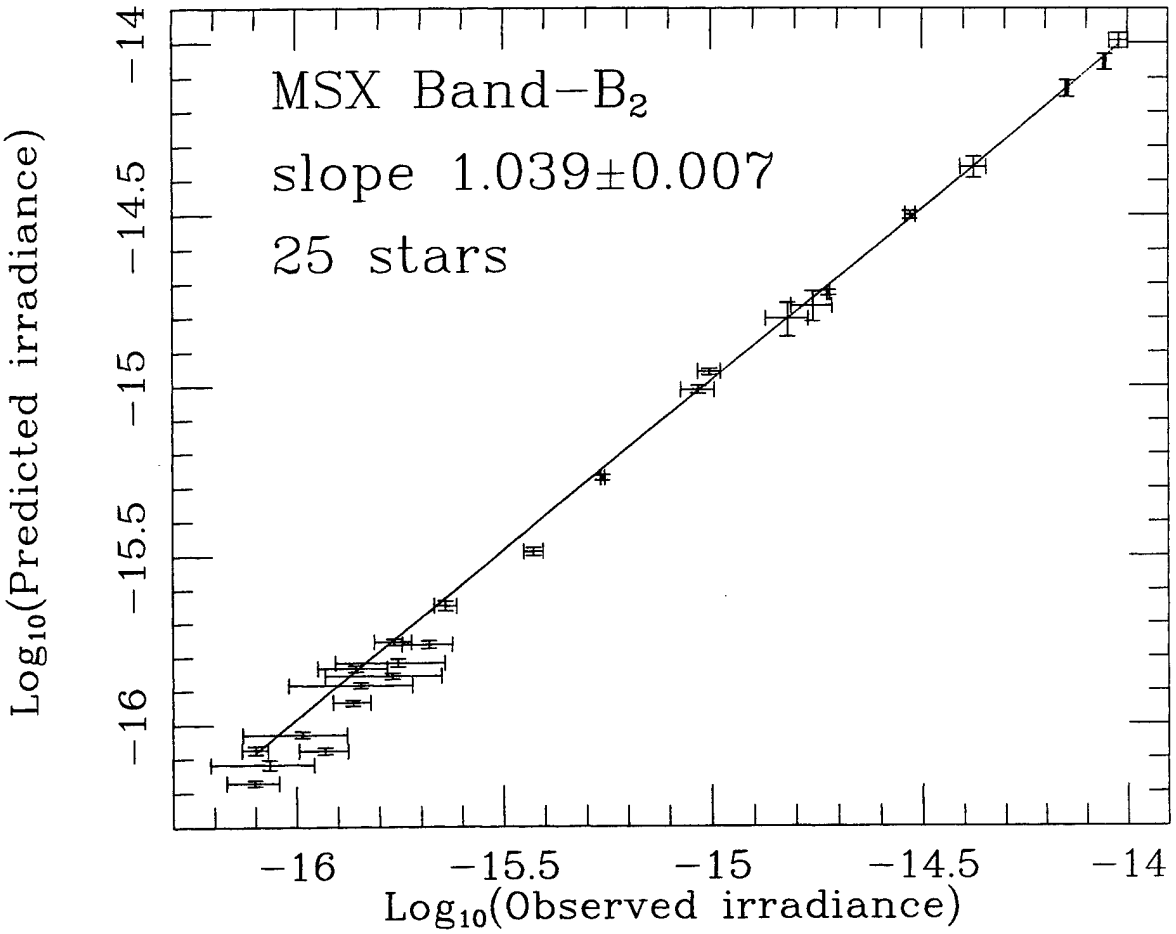

Figure A-5: As in Figure A-3 but for Band-B_2 Measurements.

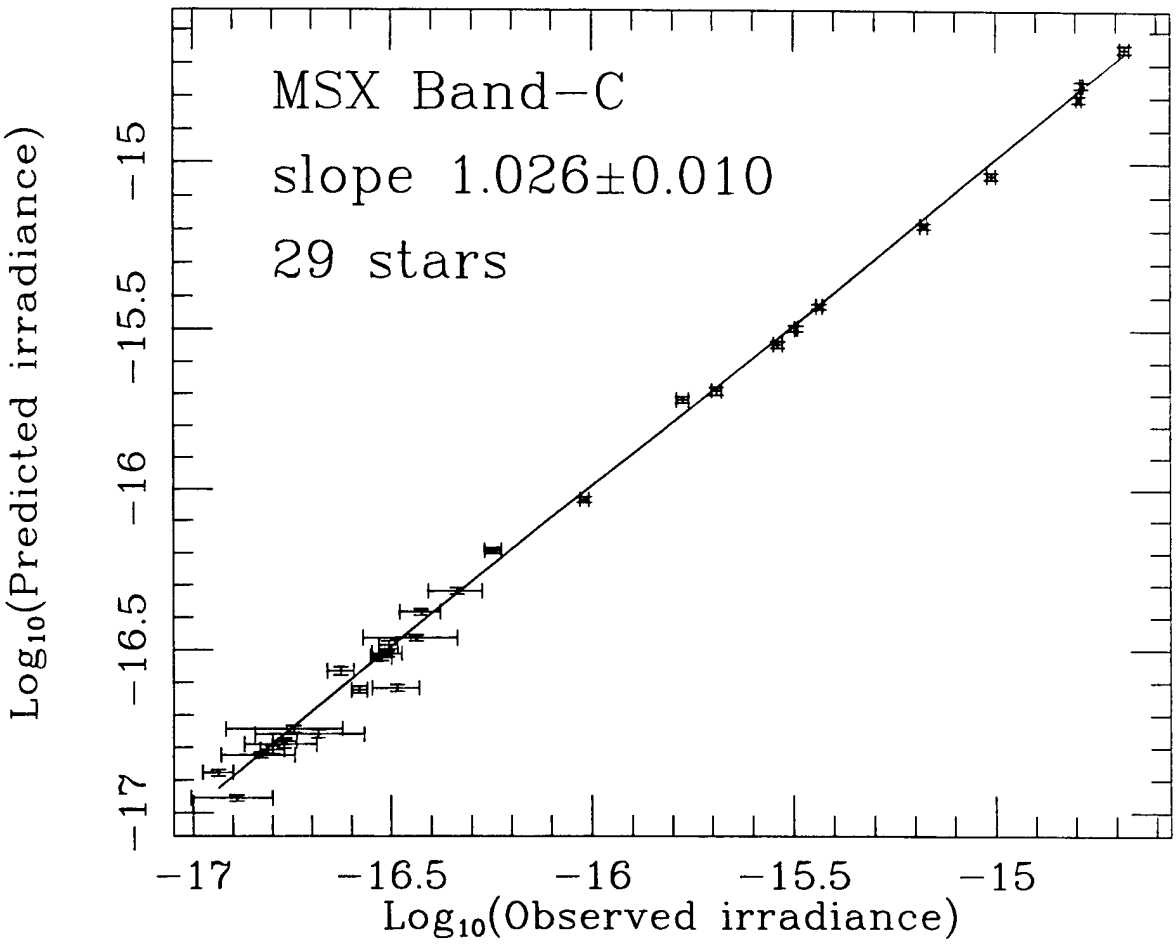

Figure A-6: As in Figure A-3 but for Band-C Measurements.

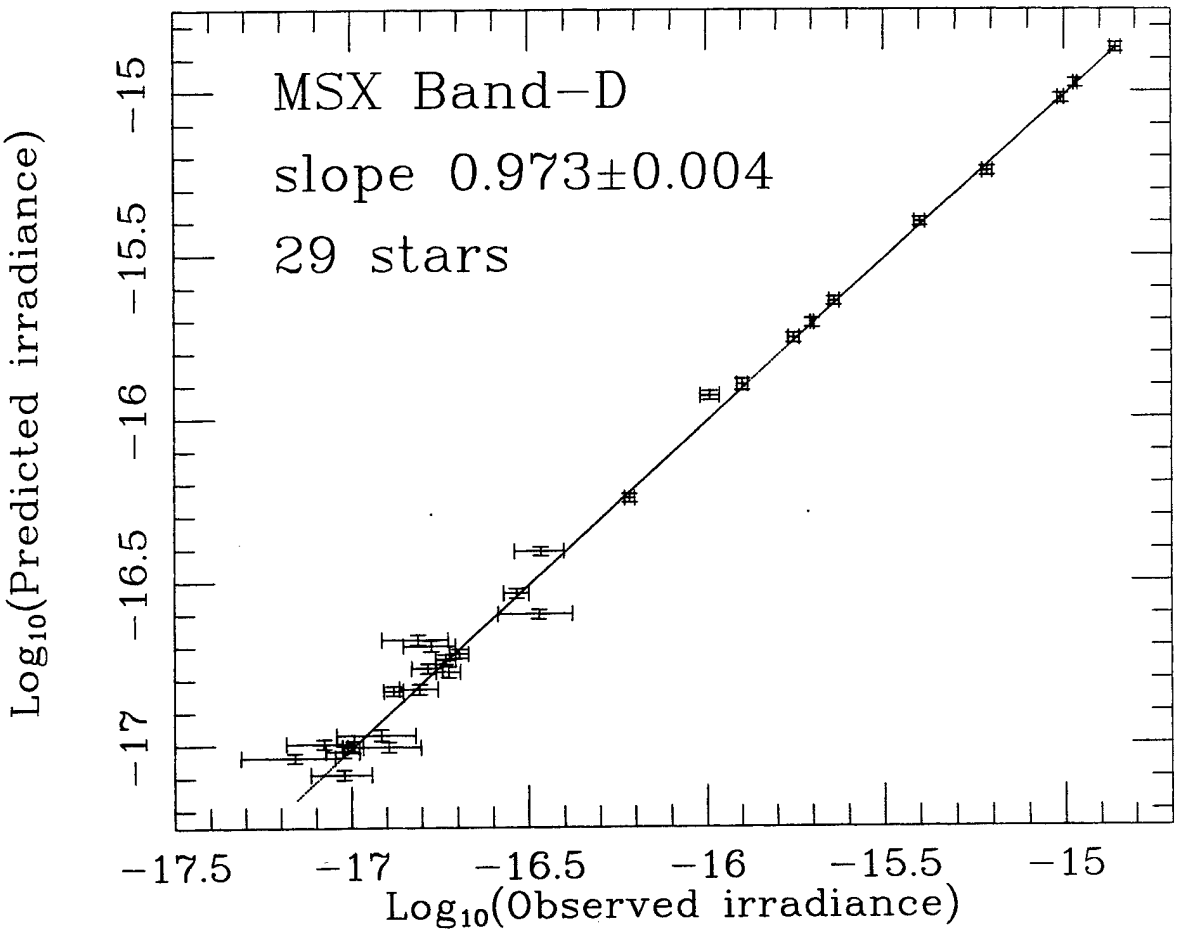

Figure A-7: As in Figure A-3 but for Band-D Measurements.

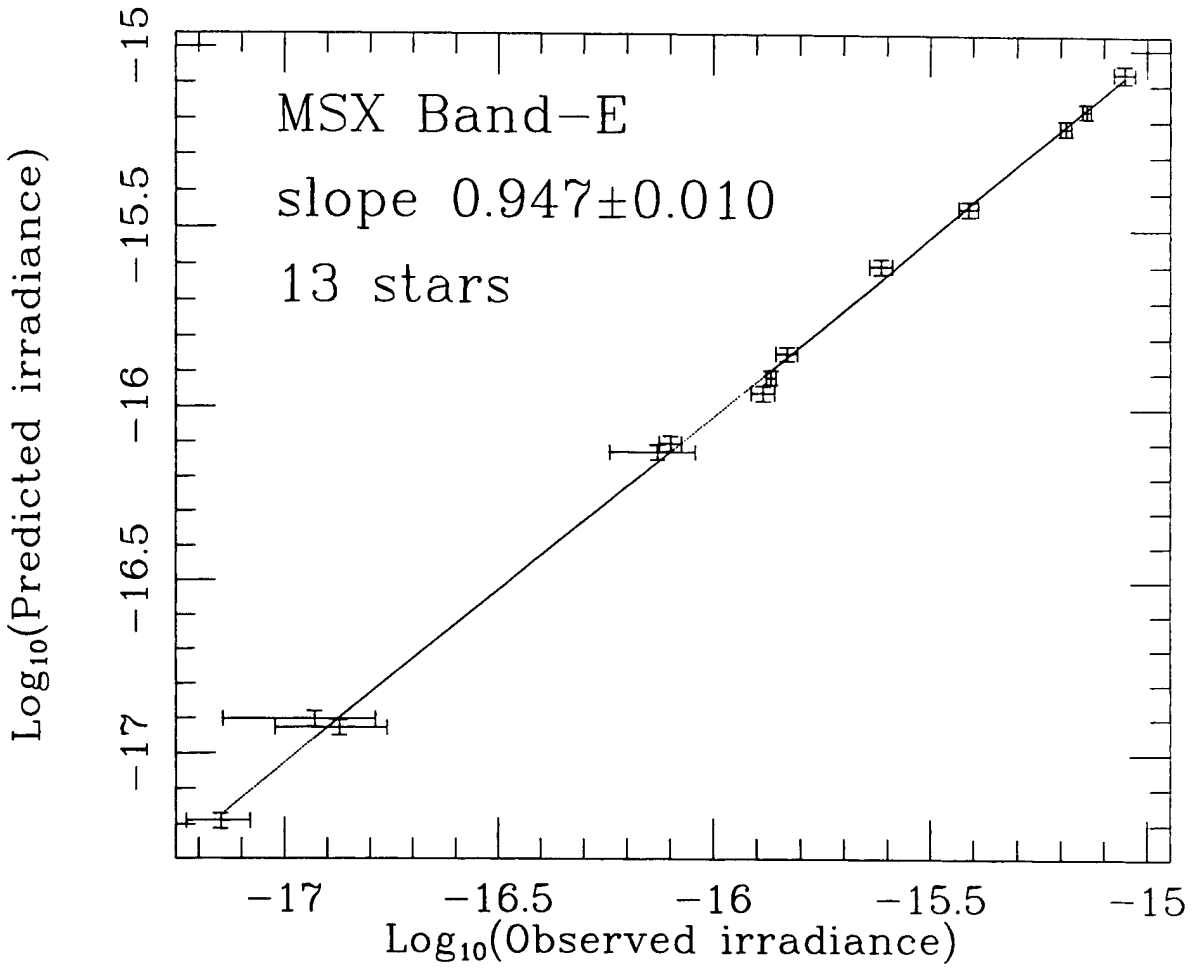

Figure A-8: As in Figure A-3 but for Band-E Measurements.

Appendix B.

Radiometric Validation of the Midcourse Space Experiment's (MSX) Point Source Catalogs & the MSX Properties of Normal Stars

Martin Cohen

Vanguard Research, Inc., Suite 204, 5321 Scotts Valley Drive, Scotts Valley, CA 95066 and

Radio Astronomy Laboratory, 601 Campbell Hall, University of California, Berkeley, CA 94720

Electronic mail: mcohen@astro.berkeley.edu

Peter L. Hammersley

Instituto de Astrofisica de Canarias, La Laguna, Tenerife, Canary Islands

Electronic mail: plh@ll.iac.es

Michael P. Egan

AFRL/VSBC, 29 Randolph Rd., Hanscom AFB, MA 01731

Electronic mail: Michael.Egan2@hanscom.af.mil

ABSTRACT

We describe our methods to validate the absolute calibration of the infrared (IR) radiometry of the MSX Point Source Catalog, version 1.2 (PSC1.2). These are based upon stars drawn from our current all-sky network of absolute calibrators, and other stars that also support the calibration of ESA's Infrared Space Observatory (ISO) and of several other satellites. All four of MSX's mid-IR bands are entirely consistent with this network, but the two narrowest bands (near 4.3 μm) are discrepant by a few percent. This paper probes radiometry of fainter stars than those validated by an independent study of the primary and secondary MSX standards by Cohen et al. (2000). To provide the user of the PSC1.2 with a basis for comparison, we derive the IR properties of normal stars from measurements by MSX's infrared focal planes.

Subject headings: infrared — absolute calibration — stars

1. INTRODUCTION

The US Midcourse Space Experiment (MSX: Mill et al. 1994) was launched in spring 1996. An excellent overview of MSX and its sensors is given in the Johns Hopkins APL Technical Digest (1996). Details of the astronomy carried out on MSX using the SPIRIT-III (Spatial InfraRed Imaging Telescope-III) can be found in Price et al. (1996), and the PSC1.2 is accompanied by an Explanatory Guide that describes the process of constructing the PSC1.2 from raw SPIRIT-III data (Egan et al. 1999). The areal coverage of the PSC1.2 derives from two experiments on the MSX; the survey of the entire Galactic plane between +5° and -5° of latitude (~9% of the sky); and the ~4% of the sky unobserved by IRAS (mostly at high Galactic latitudes).

The philosophy of calibrating SPIRIT-III involves a tripartite approach, blending the results of ground calibration and instrument characterization pre-launch with on-orbit determination of point response functions, measurements of a set of established IR calibration stars, and rapid scanning observations of a series of emissive spheres ejected 5 times during the roughly 9 month cryogenic lifetime of MSX. Each of these independent approaches contributes to the overall calibration of SPIRIT-III and a technique combining all three into a globalized MSX calibration is being applied by the Data Certification and Technology Transfer team of the MSX program (Murdock et al. 2000). Indeed, a great deal of the time spent on astronomy with MSX was devoted to calibrations of various kinds. A detailed discussion of this overall strategy was presented (Murdock 1997) to the ISO Science Team during the cryogenic life of ISO, to provide an explanation for the absolute basis of those same stellar spectra that underpin the absolute calibration of three of the four ISO instruments.

The fact that one begins with a single star, or even a set of calibration stars, does not necessarily imply that the implementation of satellite observations of these on orbit

reference objects within a data pipeline leads to the correct irradiances of the wide variety of sources measured by that satellite. The clearer that the design of the calibration philosophy is, the more likely it is that such will be the case but there is no substitute for *post facto* validation. The calibration framework that we have constructed can be represented by an inverted pyramid with Sirius and Vega at its apex as primary standards (Cohen et al. 1992a), extended by a tier of bright K- and early-M giants (Cohen et al. 1992b, 1995, 1996), and finally broadening into 422 fainter stars (Cohen et al. 1999). The entire ensemble of 1–35 μm absolute spectra and its supporting photometry is self-consistent. In the near- and mid-IR, DIRBE used Sirius as its basis star, from which it created its own empirical set of 92 calibrators around the sky (Mitchell et al. 1996). Cohen (1998) demonstrated that DIRBE had correctly maintained the integrity of this absolute calibration through analysis of DIRBE's own observations of this same set of bright K- and M-giants.

The purpose of this paper is to subject MSX's PSC1.2 to the same rigor. In Sections 2 and 3 we describe the sets of stars used to test the irradiance scale of the PSC1.2 over a wide range of values. Having verified the accuracy of PSC1.2 irradiances in Section 4, we proceed in Section 5 to derive the colors of normal stars by comparing PSC1.2 with the Hipparcos and Tycho archives and creating optical-IR color-color plots. Finally, we examine the Hertzsprung-Russell diagram for stars of different luminosity class in MSX's most sensitive IR band, "Band-A" hereafter, [8.3], where we designate each band by [λ], where λ is the isophotal wavelength for Vega in that band, and λ is given in microns.

2. SPIRIT-III AND ITS CALIBRATION STARS

Table 1 summarizes the "zero magnitude" attributes of the 6 SPIRIT-III bands, on the basis of integration over our fundamental, calibrated, Vega spectrum (Cohen et al. 1992a).

The stars examined repeatedly by SPIRIT-III to provide the on-orbit calibration are α CMa, α Lyr, α Boo, α Tau, β Peg, and β Gem. These six stars offer fiducial irradiances that span a range of only a factor of $\sim$20, and primarily sample the top end of the dynamic range for most SPIRIT-III bands, although the longest, "Band-E", is quite faint for α Lyr. Egan et al. (1999: their Table 3) present the irradiances that result after integration of the 6 relative spectral response (RSR) curves for the 6 SPIRIT-III bands over our published spectra for these primary and secondary stars used to calibrate MSX.

3. STAR SELECTION

Many calibration experiments on MSX involved use of the "scan mirror" - a device in the optics of SPIRIT-III that could rapidly scan a source across the active columns of all the IR focal planes. However, the PSC1.2 is constructed from long scans across the sky in which this mirror was in its fixed position. Therefore, to verify the calibration of PSC1.2, we have confined our selection of stars to objects that are actually in the PSC1.2; i.e. they have passed through the identical optical train and Celestial Automated Processing pipeline as the roughly one third of a million sources in this data set.

Two different samples were sought. The first consists of all those stars among the 422 calibrated template spectra that constitute the body of Cohen et al.'s (1999) all-sky network. The second was drawn from the several hundred stars with a wide variety of spectral types that were assembled as part of ISO's "Ground-Based Preparatory Programme" (GBPP: van der Bliek et al. 1992), and were observed by Hipparcos. Kurucz model spectra were produced for these stars using the method described by Hammersley et al. (1998), selected on the basis of temperature and metallicity information for the individual stars. Each model was then normalized to 2.2-μm photometry. It is those normalized models that we have used for our second set of calibrated spectra.

Note that all the stars used in the present paper to validate MSX's radiometry are fainter, often substantially, than the bright primary and secondary stars (first and second tiers of our framework) independently analyzed by Cohen et al. (2000) in their parallel study of the another, formal, absolute calibration experiment carried out on MSX.

3.1. Calibrated Template Stars

Although most of the Cohen-Walker-Witteborn bright K- and M-giants were observed by some experiment aboard MSX, often with the scan mirror active, though sometimes in mirror-fixed mode (cf. Egan et al. 1999), none appear in the PSC1.2. However, the self-consistency of the network enables us just as readily to probe the accuracy of PSC1.2. irradiances using fainter stars. Sixteen of the 422 templated stars appear in the PSC1.2: HD numbers 5234, 34334, 48433, 49293, 55775, 59381, 61294, 63697, 70555, 89388, 89682, 107274, 170693, 183439, 189276, and 216032. Not all of these 16 stars were detected in all 6 bands but they do provide values for irradiance that span a range of a factor of 3–8. That we see so few members of this all-sky network of 422 stars is explained by its relatively uniform sky distribution, the heavy concentration of PSC1.2 to the Galactic plane, and the fact that PSC1.2 in its entirety samples only ~13% of the whole sky.

3.2. Kurucz Models Supporting ISO

Two considerations caused us to widen the types of star sampled. The first was a general issue, namely the need to enlarge the dynamic range in irradiance investigated in all 6 bands. The second relates specifically to the two short-wavelength, narrow bands near 4.3 μm, which were selected precisely because they lie in the terrestrial CO_2 bands (to address down-looking objectives for MSX). Although our bright K- and M-giants were

observed both from the Kuiper Airborne Observatory (KAO) and from satellites (the IRAS Low Resolution Spectrometer: LRS), there can still be gaps, primarily between about 4.2 and 4.4 μm, because this CO_2 absorption is still saturated from KAO altitudes. These cool giants also show CO fundamentals near 4.5 μm and their spectra are rising (in $\lambda^4 F_\lambda$ space) rapidly from this fundamental to the quasi-continuum. To avoid possible problems with interpolation of these composite spectra across any narrow gaps, we also wanted to use some stars that lacked the CO band, suggesting the usage of much warmer stars. (Note that the associated CO_2 band between about 14 and 16 μm, however, is covered entirely by the IRAS Low Resolution Spectrometer.) These two considerations caused us to seek A, F, (and G) stars whose spectra are based on model atmospheres, so that they have continuous, featureless energy distributions through Bands B_1 and B_2.

We found 103 ISO/Hipparcos stars matched in the PSC1.2. Although a very wide variety of spectral types was used to support ISO's needs, we do not believe that *any* supergiants should be utilized for radiometric checks because of the likelihood that these have stellar winds with free-free emission over and above their photospheric radiation (if of types B, A, F, or G), and/or emission by warm circumstellar dust (if of types K or M). Both these processes can weaken photospheric absorption features, such as the CO and SiO fundamentals, and distort the mid-IR energy distributions by dust emission features. Consequently, we excluded all supergiants from these radiometric checks. We also rejected all K- and M-type dwarfs and giants because the Kurucz models do not include the SiO fundamental band near 8 μm and this is prominent in these stars.

4. THE RADIOMETRIC CHECKS

The actual radiometric checks consisted of forming the ratio of MSX's measured irradiance, on a given star and band, to that predicted from the integration of the RSR over

the appropriate templated, or modeled, spectrum. The PSC1.2 contains both irradiances and the uncertainties in these quantities. We later combined data within each, and from both, of the two sets of stars, treating every such ratio using inverse-variance weighting.

Table 2 presents the results of these comparisons, distinguishing the two sets of stars used, and incorporating the total range in irradiance probed by each set in every band.

5. SPIRIT-III ATTRIBUTES OF NORMAL STARS

To explore how normal stars appear to MSX, the PSC1.2 was cross-correlated with both the Hipparcos output catalog (van Leeuwen et al. 1997) and the Tycho catalog (Hoeg et al. 1997). The Tycho magnitudes provide a homogeneous photometry set covering the whole sky, complete to over 99.9% at V_T=10. Therefore, all of the normal stars detected by MSX will be included in this catalog. The Hipparcos catalog has fewer sources, but provides far more information on those, notably spectral types and luminosity classes. In the following, V_T and B_T, rather than Johnson V and B, will be used, as these were the measured quantities.

When cross-correlating MSX positions with Hipparcos or Tycho it was found that 50% of the matches in position were within 3″ and 90% of the matches within 7.8″. These figures are consistent with the quoted accuracy for MSX PSC 1.2 (Egan et al. 1999: their Table 14) of 1σ in-scan of ~2.2″, and cross-scan of ~1.9″. Therefore, for the comparison work, a match was assumed if the positions agreed to within 7″. This does remove some real matches but it reduces the number of false matches to acceptably low levels. The correlation with Hipparcos found 6500 matches, of which 0.25% will be false, and that with Tycho 25500 matches, of which 0.75% will be false. The numbers of false matches were quantified by shifting the MSX coordinates by 1′ and rerunning the cross-correlations.

When correlating the visible catalogs with MSX, there will be a number of selection effects due to the different limiting magnitudes and wavelength ranges. The PSC1.2 is primarily a low-latitude survey and the majority of the MSX sources will be deep within the Galactic Plane. Furthermore, these sources often have large IR excesses due to dust shells; otherwise they would not have been detected, particularly at the longer wavelengths. But at visible wavelengths, these sources are very faint and do not appear in the Hipparcos or Tycho catalogs. This explains why fewer than 8% of the MSX PSC1.2 sources have matches with Tycho. MSX is generally complete to magnitudes of [8.3]=$6.^m2$, [12.1] and [14.6]=$4.^m9$ (cf. Egan et al. 1999, their Figs. 29-38, after allowance for Malmquist bias in the two faintest bins at the peak of the counts' distributions). Therefore, it detects only the very closest, low-luminosity stars. The spatial distribution of matched sources shows little correlation with Galactic longitude.

In the following discussion of figures, we note that all sources plotted have PSC1.2 quality flags of 3 or 4 ("good" or "excellent": cf. Table 5 of Egan et al. (1999) for the quantification of these criteria).

Figure 1 shows the plots of V_T-[8.3] against spectral type for the five basic luminosity classes, together with a plot for all stars with a spectral type that lack a luminosity class. Every star was individually corrected for extinction in these plots, according to its Hipparcos-determined distance, using A_V=0.62 mag kpc^{-1}. Table 3 summarizes these extinction-corrected plots in tabular form, giving median color indices. Figure 1 is is not repeated for the other filters because normal stars (without infrared excesses) have colors between Band-A and any other MSX filter that are very small, because all MSX wavelengths are in, or close to, the Rayleigh-Jeans domain for these stars. In general, there are no surprises in these diagrams but the number of B- and A- stars of luminosity classes III-V with significant infrared excesses is noteworthy. This is redolent of the same phenomenon

found for the IRAS properties of normal stars (Cohen et al. 1987) at 12 μm, which was attributed to illumination of nearby interstellar material and excitation of polycyclic aromatic hydrocarbons (PAHs) by stellar ultraviolet radiation. The same explanation can probably be applied to at least some of the B-and A-dwarfs and giants with unusually large V_T-[8.3] in Figure 1, particularly given the location of the strongest "unidentified IR" emission bands, in Band-A. Note also that excesses are much more common among supergiants (luminosity classes I and II) of *all* spectral types, no doubt because the often strong stellar winds in these objects produce significant amounts of free-free emission, above photospheric radiation. The dispersion in these excesses arises from the variations in mass loss rate from star to star. Again, we emphasize the importance of *avoiding supergiants of any type as calibration stars.*

Figure 2 shows the plots of B_T-V_T *vs.* V_T-[λ] based on the matches with the Tycho catalog. (The plot for [8.3] uses smaller points due to its fainter limiting magnitude and substantially greater number of stars detected.) In the [8.3] plot, early K-giants lie near V_T-[8.3]$\sim$2.5, B_T-V_T $\sim$1; main-sequence stars lie along the stripe to the lower left of this; M-giants are above and to the right.

Figure 3 shows [8.3]-[λ] *vs.* B_T-V_T for sources matched with the Tycho catalog. For normal stars, [8.3]-[λ] should be close to zero and a number of such sources appear in the [8.3]-[12.1] and [8.3]-[14.6] plots. The denser clumps at B_T-V_T=2 are the M-giants. We note the presence of a number of sources with [8.3]-[12.1]$\sim$0.8 for all values of B_T-V_T from 0 to 3. For B_T-V_T >1 these objects appear slightly redder in the [8.3]-[14.6] plot and very red in the [8.3]-[21.3] plot, suggesting that they are real rather than due to instrumental effects. We identify these with AGB M-stars, where the silicate features above the continuum contribute to the greater brightness in [12.1] as compared with both [8.3] and [14.6], and to the [8.3]-[21.3] color indices. A number of objects with B_T-V_T <1 show very large apparent

color indices. While it is possible that some of these may correspond to valid 8.3-μm stellar detections poorly merged with neighboring, real 12.1-μm and 14.6-μm sources, we suspect many are real. We reach this conclusion by five independent routes. First, many of these sources have high signal-to-noise ratios in bands CDE. Second, all have PSC1.2 quality flags of 3 or 4, in all detected MSX bands. Third, many show a progression of increasing color excess with wavelength, roughly consistent with ensembles of cool ($\sim$150-250K) dust particles. Fourth, there is a tendency for hotter stars to have larger excesses, particularly at 21.3 μm. Finally, there is precedent for this effect for IRAS sources associated with hot stars that illuminate nearby interstellar clouds (Cohen et al. 1987), as described above for Figure 1. All these characteristics militate against dismissing these sources as mere artifacts.

Figure 4 presents the HR diagram taking the distance and V_T from the Hipparcos catalog and [8.3] from MSX, and applying the identical corrections for extinction as were made for Figure 1 and Table 3. Note that we have made no attempt to correct the HR diagrams for any Malmquist bias inherent in the Hipparcos-determined distances. The plot was repeated 4 times, taking different limiting distances. At a distance of 600 pc, the uncertainty in parallax corresponds to an error in distance of about 40%. As expected, the lower luminosity, main-sequence stars dominate at the closest distance. By 50 pc, the early-K-giants ($M_{[8.3]}$=-1.6, V_T-[8.3]=2.5) are present and, by 200 pc, these constitute a dense blob, indicating that they are by far the most common giants. At the furthest distance, the more luminous, very red sources are well-established, e.g. AGB stars, Miras, etc.

6. CONCLUSIONS

We have validated the radiometric accuracy of MSX's PSC1.2 using two distinct sets of stars previously established as absolute calibrators for ISO and MSX, and extracted from the PSC1.2 data set. MSX Bands ACDE are in accord with expectation. The two narrow bands, B_1 and B_2, are slightly discrepant from expectation so that PSC1.2 yields irradiance ratios in the sense (measured/predicted) a few percent less than unity. This effect will be corrected in the version 2 release of the MSX PSC (now under construction). We have plotted and tabulated the observed optical-to-MSX colors of normal stars of all spectral types and luminosity classes, and have presented an HR diagram for absolute [8.3] magnitude.

MC acknowledges support for these calibration efforts, through Air Force Research Laboratory, by Dr. Stephan Price under contract F19628-98-C-0047 with VRI, and partial support via NASA-Ames through Co-Operative agreement NCC 2-142 with Berkeley.

REFERENCES

Cohen, M. 1998, Spectral Irradiance Calibration in the Infrared. IX. Calibrated Stellar Spectra using DIRBE Radiometry, *Astron.J.*, **115**, 2092

Cohen, M., Schwartz, D., Chokshi, A., & Walker, R.G. 1987, IRAS Colors of Normal Stars, *Astron.J.*, **93**, 1199

Cohen, M., Walker, R.G., Jayaraman, S., Barker, E., & Price, S.D. 2000, Spectral Irradiance Calibration in the Infrared. XII. Radiometric measurements from the Midcourse Space Experiment (MSX), *Astron.J.*, **121**, 1180

Cohen, M., Walker, R.G., Barlow, M.J., & Deacon, J.R., 1992a, Spectral Irradiance Calibration in the Infrared. I. Ground-Based and IRAS Broadband Calibrations, *Astron.J.*, **104**, 1650

Cohen, M., Walker, R.G., Carter, B., Hammersley, P., Kidger, M., & Noguchi, K., 1999, Spectral Irradiance Calibration in the Infrared. X. A Self-Consistent Radiometric All-Sky Network of Absolutely Calibrated Stellar Spectra, *Astron.J.*, **117**, 1864

Cohen, M., Walker, R. G., & Witteborn, F. C. 1992b, Spectral Irradiance Calibration in the Infrared. II. Alpha Tau and the Recalibration of the IRAS Low Resolution Spectrometer, *Astron.J.*, **104**, 2030

Cohen, M., Witteborn, Bregman, J. D., Wooden, D.H., Salama, A., and Metcalfe, L. 1996, Spectral Irradiance Calibration in the Infrared. VI. 3-35 Micron Spectra of Three Southern Standard Stars, *Astron.J.*, **112**, 241

Cohen, M., Witteborn, F.C., Walker, R.G., Bregman, J.D., & Wooden, D.H. 1995, Spectral Irradiance Calibration in the Infrared. IV. 1.2-35 Micron Spectra of Six Standard Stars, *Astron.J.*, **110**, 275

Egan, M.P. et al. 1999, The Midcourse Space Experiment Point Source Catalog Version 1.2 Explanatory Guide, Air Force Research Laboratory Technical Report, AFRL-VS-TR 1999-1522, ADA 381933

Hammersley, P.L. et al. 1998, Infrared standards for ISO. I. A new calibration of mid infrared photometry, *Astron. & Astrophys. Suppl.*, **128**, 207

Hoeg, E. et al. 1997, The TYCHO Catalogue, *Astron. & Astrophys.*, **323**,57

Johns Hopkins APL Technical Digest 1996, Midcourse Space Experiment: Overview, **17**,1

Mill, J., O'Neil, R. R., Price, S. D., Romick, G. J., Uy, O. M., & Gaposchkin, E. M. 1994, Midcourse Space Experiment: Introduction to the Spacecraft, Instruments and Scientific Objectives, *AIAA*, **31**, 900

Mitchell, K. J. et al. 1996, Infrared Point Source Photometry With DIRBE: Instrument Gain Stabilization and Variable Star Monitoring, in Unveiling the Cosmic Background, ed. E. Dwek (AIP, CP 348), p.301

Murdock, T.L. 1997, Calibration Certification for SPIRIT III on MSX, ISO Calibration Working Group, meeting no. 21, Vilspa, 12 March 1997

Murdock, T.L. et al. 2000, Globalization of the MSX Calibration, in preparation

Price, S.D. et al. 1996, Astronomy of the Midcourse Space Experiment, Proc. IAU Symp. 179, eds. B. J. McLean et al., Kluwer Academic, p.115

van der Bliek, N.S. et al., 1992, Standard stars for the Infrared Space Observatory, ISO, *ESO messenger*, **70**, 28

van Leeuwen, F., Evans, D. W., Grenon, M., Grossmann, V., Mignard, F., Perryman, M. A. 1997, The HIPPARCOS mission: photometric data, *Astron. & Astrophys.*, **323**, 61

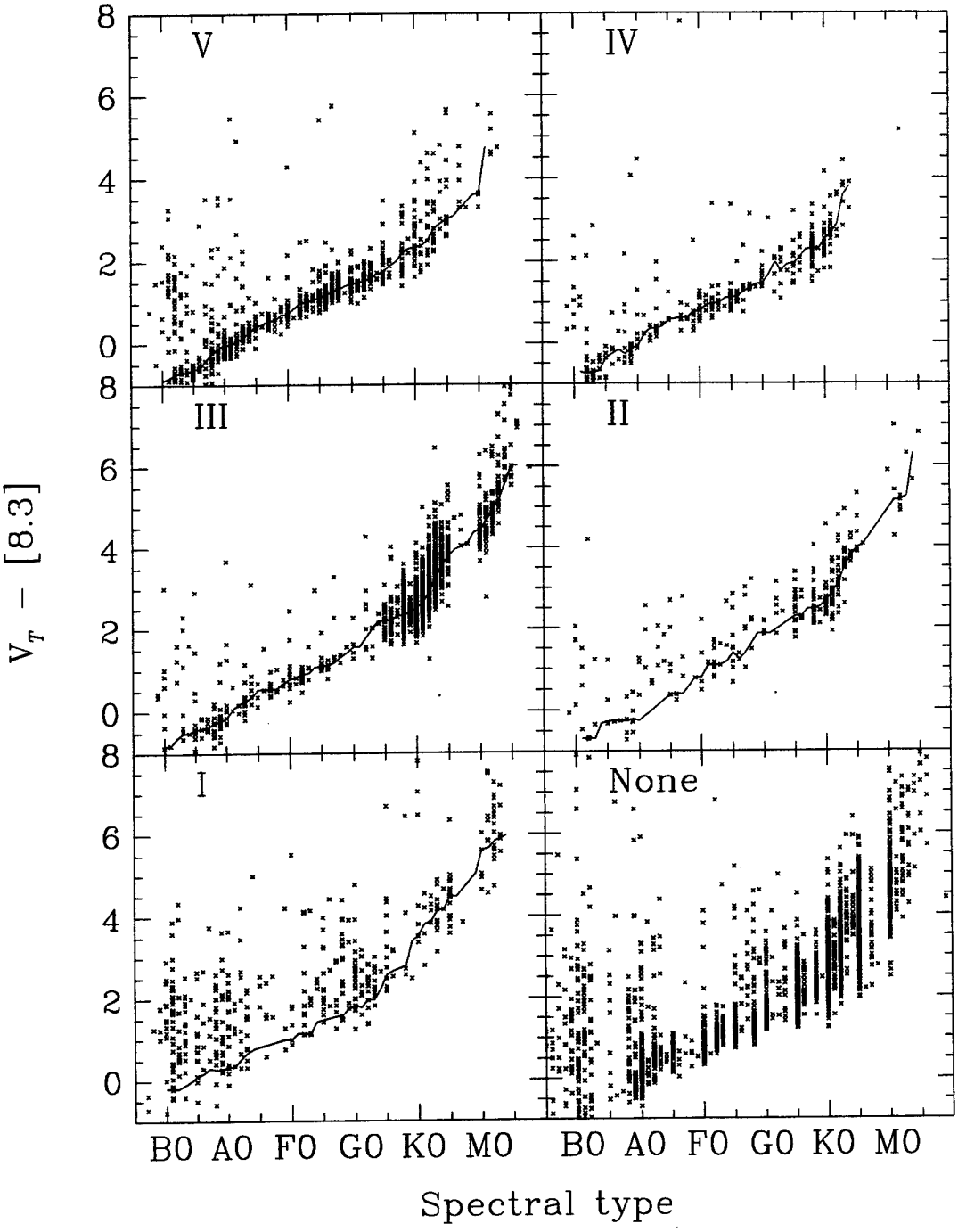

Figure B-1. V_T-[8.3] as a Function of Spectral Type and Luminosity Class for Stars in the Hipparcos Catalog.

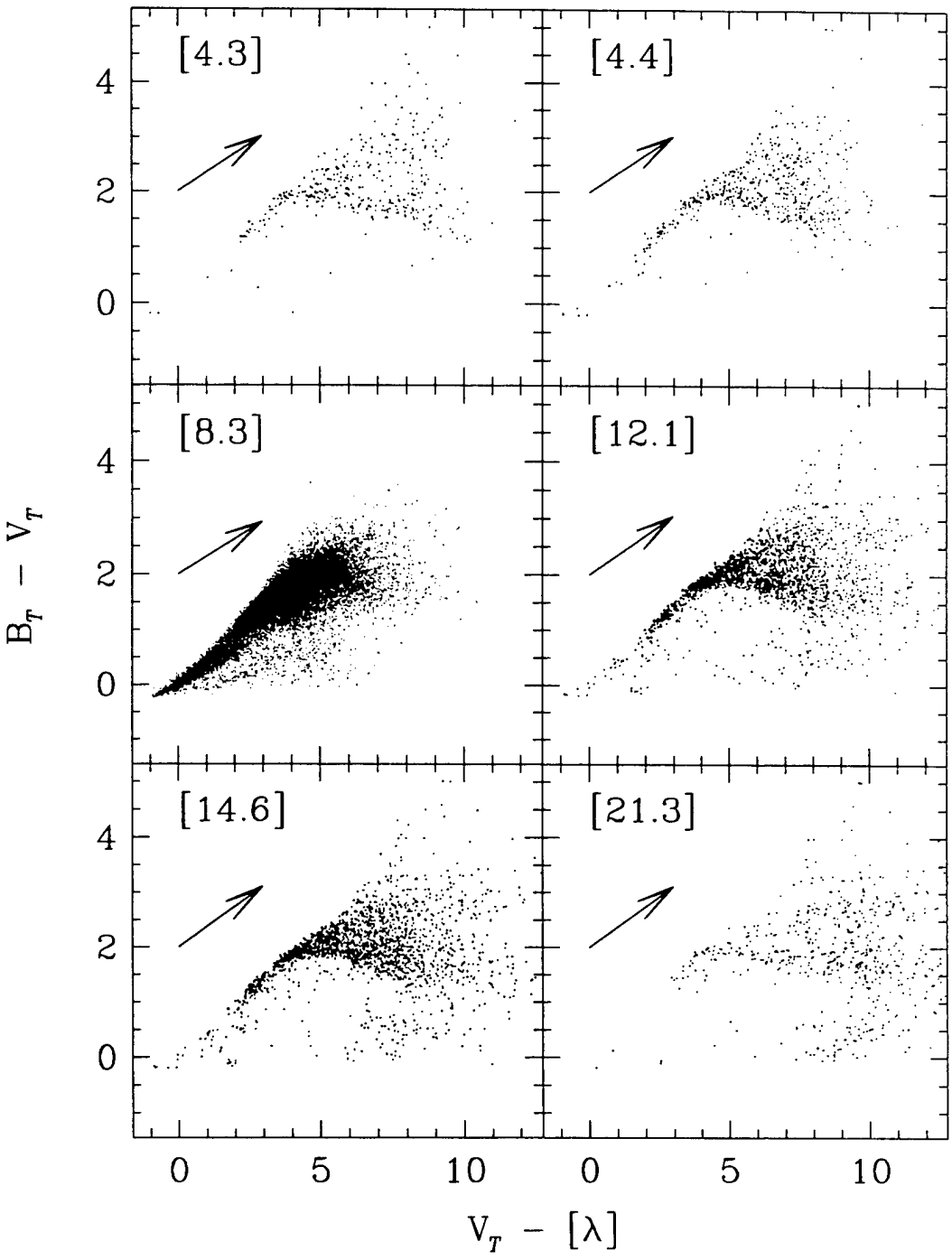

Figure B-2. B_T-V_T Against V_T-[λ] for Stars in the Tycho Catalog, for Each of the 6 MSX Bands; dots used for the large number of stars plotted in the V_T-[8.3] diagram are much smaller than in the other diagrams. The arrow indicates the effect of a reddening of 3 magnitudes.

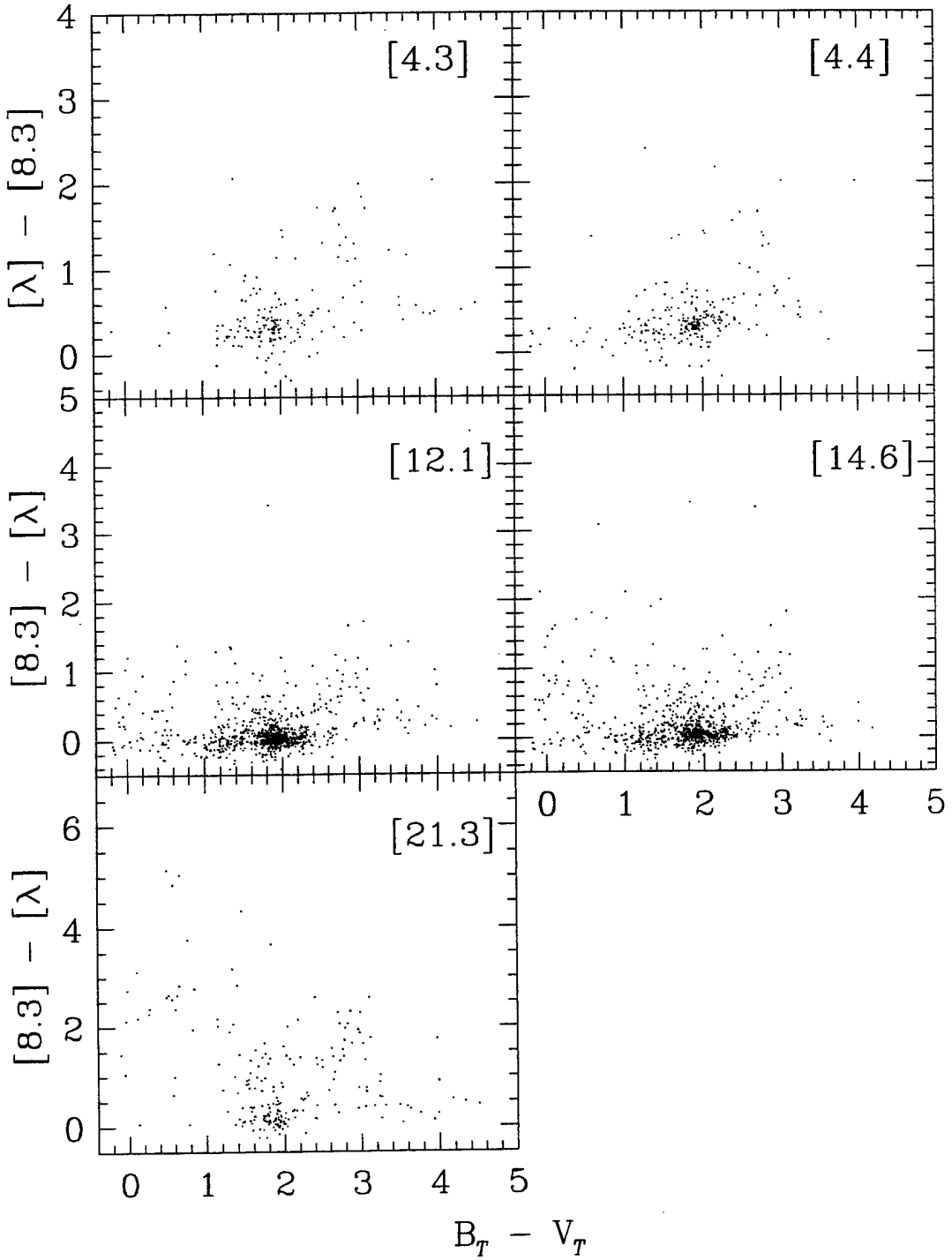

Figure B-3. MSX Color Indices With Respect to [8.3] as a Function of Observed B_T-V_T Index for Tycho Stars.

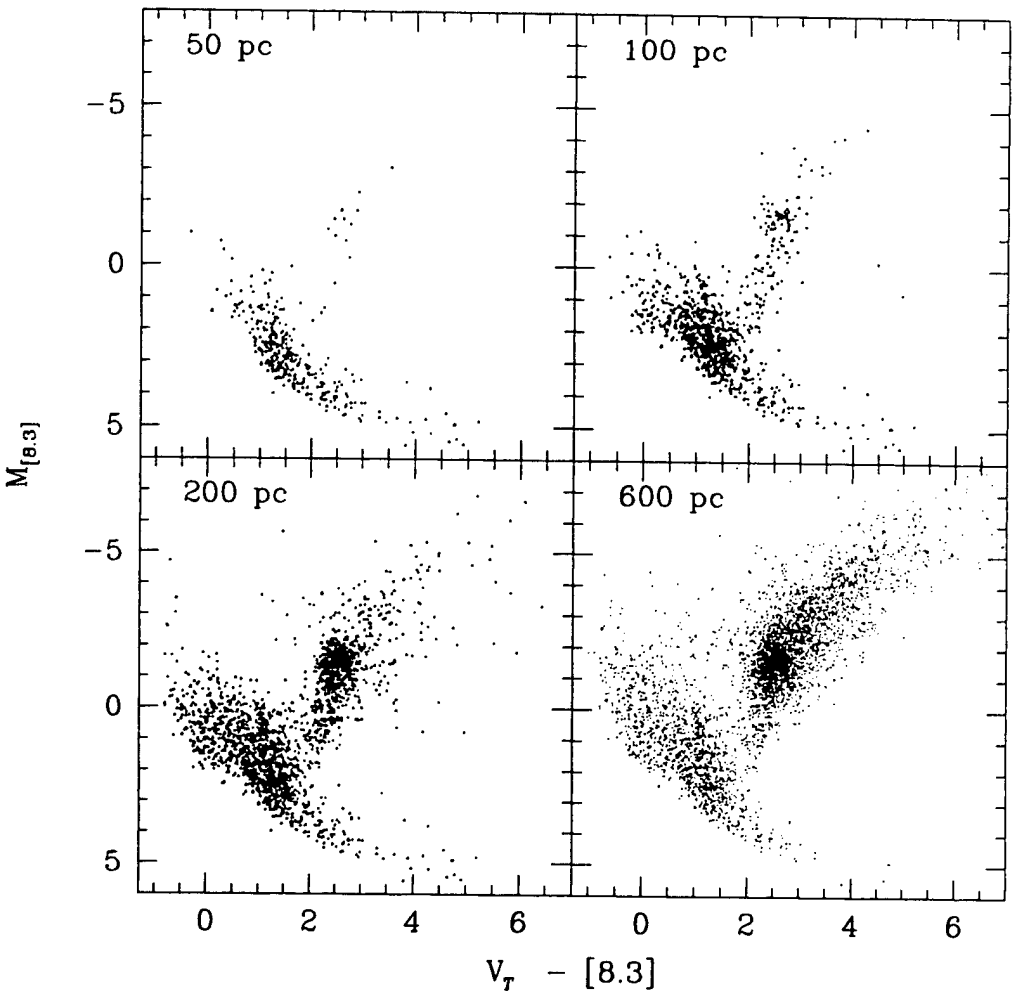

Figure B-4. Absolute Magnitude at 8.3 μm as a Function of Extinction-Corrected V_T-[8.3] Index for Stars out to Distances to 50, 100, 200, and 600 pc, Based on Hipparcos Parallaxes. Stars in the plot for 600 pc are again represented by smaller dots to accommodate their number. Every star has been individually corrected for extinction in the plot.

Table B-1: Zero Magnitude Attributes of SPIRIT-III Bands

Filter	Bandwidth μm Uncertainty μm	In-Band W cm^{-2} Uncertainty W cm^{-2}	$F_{\lambda(iso)}$ W cm^{-2} μm^{-1} Uncertainty W cm^{-2} μm^{-1}	λ(iso) μm Uncertainty μm	Bandwidth Hz Uncertainty Hz	$F_{\nu(iso)}$ Jy Uncertainty Jy	ν(iso) Hz Uncertainty Hz
B_1	0.1036	3.279E-16	3.165E-15	4.294	1.685E+12	194.59	6.979E+13
	0.0012	6.075E-18	5.094E-17	0.0177	1.917E+10	3.134	5.818E+11
B_2	0.1794	5.364E-16	2.989E-15	4.356	2.840E+12	188.84	6.875E+13
	0.0018	9.415E-18	4.129E-17	0.0153	2.775E+10	2.606	4.866E+11
A	3.3620	8.196E-16	2.438E-16	8.276	1.402E+13	58.485	3.715E+13
	0.0124	1.225E-17	1.189E-18	0.0103	4.632E+10	0.269	8.840E+10
C	1.7205	9.259E-17	5.382E-17	12.126	3.493E+12	26.506	2.477E+13
	0.0267	1.917E-18	1.150E-18	0.0642	5.239E+10	0.556	2.593E+11
D	2.2344	5.686E-17	2.545E-17	14.649	3.109E+12	18.288	2.050E+13
	0.0669	1.767E-18	1.034E-18	0.1490	8.887E+10	0.725	4.132E+11
E	6.2440	3.555E-17	5.694E-18	21.336	4.041E+12	8.799	1.418E+13
	0.3298	1.667E-18	3.935E-19	0.3705	1.942E+11	0.577	4.598E+11

Table B-2: Ratios of Measured to Predicted Irradiance for the Three Stellar Samples.

$\lambda(\mu m)$,Band	Quantity	Template stars	ISO/Hipparcos stars	All stars
4.3	Weighted Mean(#)	0.90±0.03(11)	0.93±0.02(29)	0.92±0.02(40)
B_1	Irradiance (W cm^{-2})	4.8e-17–2.1e-16	1.6e-17–1.5e-15	1.6e-17–1.5e-15
4.4	Weighted Mean(#)	0.92±0.03(10)	0.06±0.02(35)	0.95±0.02(45)
B_2	Irradiance (W cm^{-2})	7.9e-17–5.6e-16	1.6e-17–2.2e-15	1.67e-17–2.2e-15
8.3	Weighted Mean(#)	1.05±0.01(16)	0.98±0.01(91)	1.00±0.01(107)
A	Irradiance (W cm^{-2})	1.1e-16–8.7e-16	2.0e-18–4.1e-15	2.0e-18–4.1e-15
12.1	Weighted Mean(#)	1.01±0.01(16)	0.98±0.01(39)	0.99±0.01(55)
C	Irradiance (W cm^{-2})	1.6e-17–1.0e-16	2.8e-18–4.8e-16	2.8e-18–4.8e-16
14.6	Weighted Mean(#)	1.00±0.01(16)	0.98±0.01(40)	0.99±0.01(56)
D	Irradiance (W cm^{-2})	8.2e-18–6.4e-17	1.7e-18–2.9e-16	1.7e-18–2.9e-16
21.3	Weighted Mean(#)	1.05±0.04(6)	1.08±0.03(9)	1.07±0.025(15)
E	Irradiance (W cm^{-2})	1.3e-17–4.0e-17	1.3e-17–1.8e-16	1.3e-17–1.8e-16

Table B-3: Median, Extinction-Corrected, $V_T-[8.3]$ for Each Spectral Type and Luminosity Class, Showing the Number of Hipparcos Stars Used

Lum. class	I		II		III		IV		V	
Spec. type	$V_T-[8.3]$	#	$V_T-[8.3]$	#	$V_T-[8.3]$	#	$V_T-[8.3]$	#	$V_T-[8.3]$	#
B1	-0.19	7	-0.69	5	-0.81	5	-0.70	11	-0.83	12
B2	-0.19	7	-0.69	7	-0.63	7	-0.75	19	-0.75	25
B3	....	...	-0.69	6	-0.50	7	-0.70	24	-0.67	26
B4	-0.01	4	-0.32	4	-0.49	15	-0.68	17	-0.68	35
B5	0.14	4	-0.28	3	-0.42	13	-0.37	12	-0.61	28
B6	0.14	4	-0.26	4	-0.38	18	-0.27	9	-0.59	30
B7	0.31	4	-0.26	6	-0.37	21	-0.17	10	-0.38	31
B8	0.28	8	-0.26	10	-0.25	32	-0.28	15	-0.23	39
B9	0.28	12	-0.23	10	-0.22	32	-0.14	18	-0.09	61
A0	0.34	10	-0.26	7	-0.14	23	-0.08	15	-0.02	68
A1	0.34	7	0.64	4	0.06	10	0.19	11	0.01	75
A2	0.53	7	0.64	3	0.19	13	0.34	16	0.07	69
A3	0.68	6	....	...	0.26	16	0.34	15	0.17	53
A4	0.78	4	....	...	0.36	17	0.39	14	0.30	46
A5	....	...	0.37	5	0.53	9	0.56	4	0.43	26
A6	....	...	0.38	6	0.54	12	0.58	8	0.48	30
A7	....	...	0.38	4	0.54	12	0.61	8	0.57	22
A8	....	...	....	...	0.56	13	0.61	14	0.58	25
A9	1.01	5	0.77	4	0.68	13	0.76	22	0.72	27
F0	1.01	5	0.77	5	0.78	12	0.77	23	0.72	23
F1	1.15	6	1.06	10	0.83	26	0.90	29	0.87	34
F2	1.15	5	1.08	8	0.91	22	0.97	24	1.01	38
F3	1.15	5	1.08	8	0.93	20	0.96	21	1.03	44
F4	1.44	4	1.17	7	1.08	11	1.09	32	1.08	63
F5	....	...	1.38	8	1.10	12	1.09	31	1.14	80
F6	1.63	5	1.21	8	1.12	14	1.13	34	1.20	105
F7	1.52	7	1.38	4	1.19	9	1.24	16	1.28	102
F8	1.60	9	....	...	1.33	5	1.34	10	1.33	67
F9	1.75	12	1.85	3	1.43	6	1.42	14	1.41	58
G0	1.84	11	....	...	1.57	4	1.45	9	1.47	45
G1	1.78	13	1.85	3	1.57	6	1.65	13	1.49	66
G2	1.98	11	....	...	1.59	7	1.96	12	1.54	60
G3	1.98	8	....	...	2.01	8	1.75	13	1.59	43
G4	2.25	11	2.48	16	2.21	35	1.90	17	1.71	47
G5	2.78	10	2.28	23	2.21	59	1.92	17	1.75	37

Table B-3: *continued*

Lum. class	I		II		III		IV		V	
Spec. type	V_T−[8.3]	#	V_T−[8.3]	#	V_T−[8.3]	#	V_T−[8.3]	#	V_T−[8.3]	#
G6	2.78	10	2.28	23	2.25	68	2.07	16	1.89	34
G7	2.74	5	2.46	33	2.33	236	2.26	45	2.01	30
G8	2.60	3	2.46	29	2.36	236	2.28	40	2.20	24
G9	3.39	6	2.52	47	2.41	537	2.28	57	2.30	52
K0	3.53	6	2.67	45	2.54	564	2.51	36	2.34	41
K1	3.82	8	2.86	62	2.64	723	2.63	40	2.37	51
K2	3.88	16	3.09	58	2.93	535	2.87	28	2.52	36
K3	4.16	16	3.50	40	3.29	387	3.58	13	2.80	29
K4	4.18	27	3.76	25	3.59	253	3.80	7	2.92	29
K5	4.51	16	3.96	12	3.79	131	....	...	3.03	16
K6	4.48	15	4.05	6	3.95	58	....	...	3.08	17
K7	....	...	....	...	4.45	6	....	...	3.95	6
K8	....	...	....	...	4.10	5	....	...	3.95	6
K9	5. 6	5	....	...	4.37	36	....	...	3.61	5
M0	5.62	8	5.40	3	4.44	62	....	...	3.65	4
M1	5.66	18	5.15	7	4.67	90	....	...	4.64	8
M2	5.84	17	5.15	7	4.97	80	....	...	4.75	5
M3	5.90	14	5.25	6	5.21	61	....	...	4.75	5
M4	5.99	4	6.30	3	5.58	39	....	...	....	...
M5	....	...	....	...	6.02	17	....	...	....	...

Appendix C.

AN EXPLANATORY SUPPLEMENT TO THE AIR FORCE BRIGHT SPECTRAL CATALOG, Version 1

Russell G. Walker and Martin Cohen

Vanguard Research, Inc.

Scotts Valley, CA

June 26, 2000

Submitted to the Air Force Research Laboratories

L.G. Hanscom Air Force Base, MA

Contract F19628-98-C-0047

1. INTRODUCTION

Satellites employing infrared sensors are continually being launched by space agencies, such as NASA and ESA and by the US DOD community. The successes of IRAS, ISO, IRTS, and MSX have already produced enormous infrared databases. Consequently, there must now be greater emphasis on data verification, validation, and calibration issues to assure that these data sets are of sufficient reliability for application to the quantitative design of advanced spaceborne sensors and systems. There is an urgent need not only to rationalize infrared calibration and place it in a common and well-defined context, but also to provide a network of calibrators well distributed across the sky, with a common traceable pedigree. This network should be sufficiently populated to have a member relatively close to any arbitrary direction because satellites and aircraft cannot afford major excursions in pointing to secure measurements of the few traditional calibration objects. Dynamic range, too, is an issue and such a network must include stars both fainter and brighter than today's popular "standards".

In previous work (Cohen et al. 1992-1998, Papers I-IX) we have developed a basis for irradiance calibration of space-based infrared sensors, and have fully defined the context of the calibration, and the concepts of spectral composites and templates. This work culminated in the recent publication of *An All Sky Network of 422 Infrared Calibration Stars* (Cohen et al. 1999). In the above series of papers we have described a consistent effort to provide absolutely calibrated broad and narrowband IR photometry based upon a carefully selected, IR-customized pair of absolutely calibrated stellar models for Vega and Sirius. These hot stellar models have been employed as reference spectra to calibrate the spectra of cool giants. This approach has yielded a valuable set of secondary stellar standards with calibration pedigrees directly traceable to the two primary standards. These cool giant spectra are totally unlike any blackbody, and are dominated by the fundamental absorption and overtones of CO, SiO, and water vapor. Thus the ideal (IR-bright) calibrators have significant spectral structure that is not yet adequately modeled by stellar atmospheric codes but that can be approached in a rigorous observational manner.

These (almost) entirely observed 1.2-35 μm absolute spectra of all reference stars are designated "composite spectra" (because of the method of their assembly).

Each composite spectrum has been used to create many calibrated stellar spectra, all with a traceable common calibration heritage, given a single prerequisite, namely photometry in a "well-characterized" system of filters. To achieve this goal, one must make the fundamental "template assumption", that the dereddened (for interstellar extinction) infrared spectral shape of any observed K0-M0 giant accurately represents the intrinsic spectrum of any other giant with the same two-dimensional spectral type as the composite from which the "template" is created. The adopted template (spectral shape) is reddened appropriately for the star spectroscopically unobserved in the IR, then normalized by matching the template's in-band radiometry to the measured in-band irradiances in a set of filters. The *All Sky Network of 422 Infrared Calibration Stars* referenced above was produced using this technique.

It has become clear that current demand for on-orbit calibration of space-based programs, such as SBIRS, requires brighter calibration sources than are available within the present network of 422 stars.

2.0 THE AIR FORCE BRIGHT SPECTRAL CATALOG (AFBSC)

The AFBSC is an independent set of calibrators selected to be among the IR-brightest sources in the sky. Our ultimate goal is to create complete (2-35 μm) spectra for all stars brighter than zero magnitude in the infrared. To do this we will eventually utilize IRAS Low Resolution Spectra (LRS), ISO SWS spectra, other groundbased and airborne spectral observations from the past and recent literature, as well as spectra generated by theoretical and/or empirical models. These will be normalized by means of well-characterized photometry to bring them into the photometric system described above. Candidate stars for the AFBSC are selected from the IRAS all-sky survey, the Cal. Tech. Two Micron Sky Survey, and the MSX point source catalog. For inclusion in the catalog, a star must be brighter than zero magnitude in the respective survey bands.

The brighter in the mid-infrared the required calibrators are, the greater the likelihood of encountering abnormal stars such as heavily dust-shrouded, long-period, cool variables. At the present time we lack detailed information on the spectral variations of these stars with the phase of their light curves, even for those objects whose variations are supposedly periodic. Thus, we anticipate the need to revisit this catalog in subsequent versions, once we have learned more about the characteristics of variability among these IR-bright evolved stars. Variability of the majority of the IR-bright stars is the foremost problem to be addressed if these objects are to be accepted as reliable calibrators.

2.1 AFBSC Version 1

AFBSC Version 1 is an extremely limited version that does not pretend to achieve the overall AFBSC goals either in quantity or quality of the sources. It is a result of an initial "testing of the waters" and serves a number of useful purposes. It alerts the systems designer to the potential bright calibrators that will be available to him for calibration of his spacebased, groundbased, and airborne IR systems. The irradiance levels and dynamic range possible are well-defined, even though many absolute irradiance levels have, at present, unacceptably large uncertainties for radiometric calibration. Many of these will still be useful astrometric calibrators and knowing the range of their irradiances will improve infrared acquisition by enabling discrimination among multiple objects in the field. Further, many stars are identified in this version that do have reliable and non-varying irradiances with acceptable errors, and are immediately applicable for radiometric calibration. Finally, production of this version of the catalog has identified to the authors those stars that can be readily elevated to precise calibration status, and those that will require gargantuan efforts.

2.1.1 The Stars

In Version 1.0 we have limited our choice of stars to those brighter than zero magnitude at 12□m in the IRAS PSC2. Our search returned 1638 point sources. Identification of these sources revealed that 198 were non-stellar objects (71 planetary nebulae, 126 HII regions, 1 and galaxy). In addition we removed 3 T Tauri stars and 2 young OB stars. These were deleted, reducing the input list to 1435 IR bright stars. We further required that additional infrared photometry beyond that of IRAS be found for each star in either the MSX Point Source Catalog (Egan et al. 1999) or the Catalog of Infrared Observations (CIO), Edition 5.0 (Gezari et al. 1999). Thirty-two stars that had no CIO or MSX photometry were also deleted, resulting in a final input list of 1403 stars.

2.1.2 The Spectra

All of the stellar spectra presented in Version 1.0 are a combination of observed IRAS LRS spectra (Olnon & Raimond 1986) and SKY4 library spectra (Cohen 1993,1994). The LRS spectra meaningfully cover the spectral range from 7.67 μm to 22.74 μm and consist of two independent, overlapping segments. The spectral resolution, non-uniform sample interval, and photometric noise differ in the two segments. The absolute spectral irradiance of the LRS spectrum is set by normalization of the integral of the observed spectrum, weighted by the spectral response of the IRAS 12 μm detector, to the mean irradiance observed in the IRAS 12 μm band. Thus the LRS spectrum is brought into the stellar calibration context to within the uncertainties of the noise in the integration process and the error of the IRAS 12 μm in-band irradiance, the latter usually being dominant.

SKY4 is an analytical model describing the statistical distribution of point sources within our galaxy. Its purpose is to predict counts of point sources versus limiting irradiance observed at any specific wavelength (or band) along an arbitrary, but given, line-of-sight through the

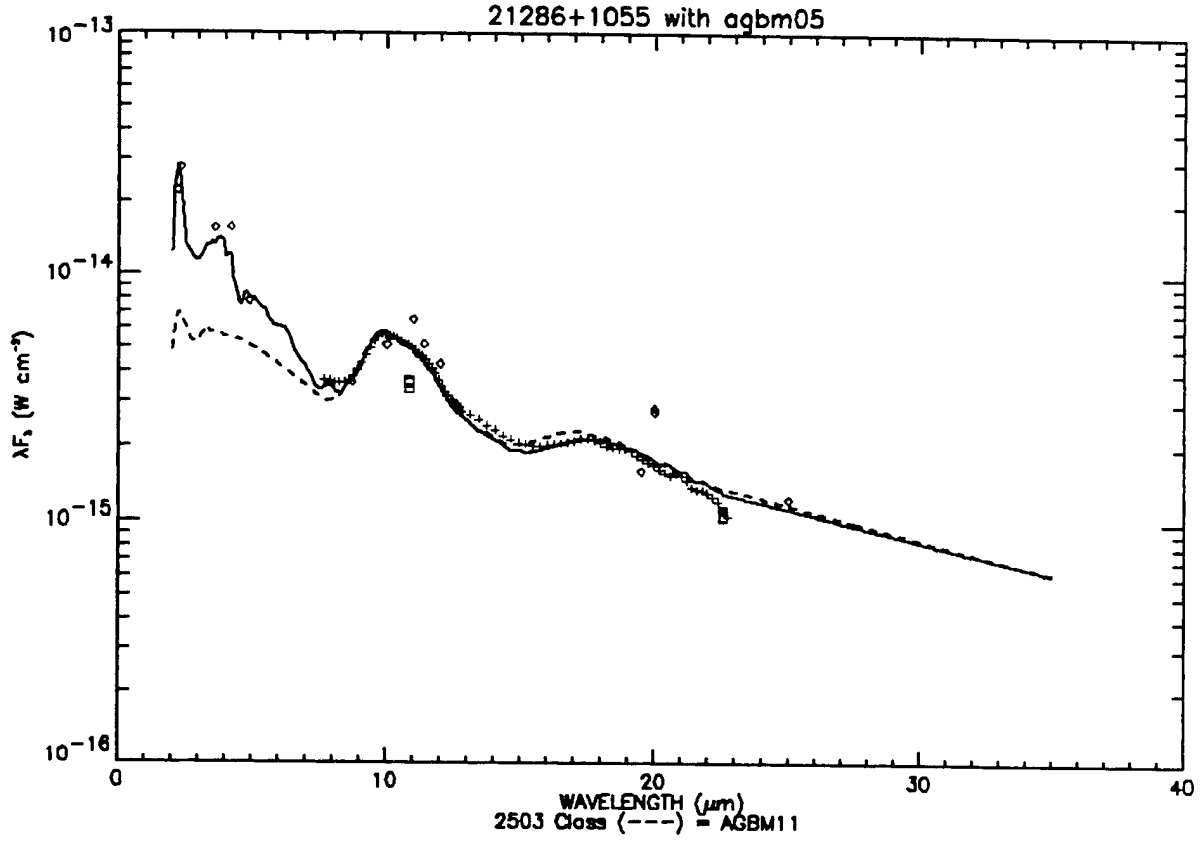

Figure C-1. LRS and Two Candidate Spectra Over-Plotted With the Available Photometry. The crosses are the LRS spectrum. The dashed curve is the SKY 4 spectrum defined by the coordinates of the star in the [12- 25], [25-60] μm color plane. The solid curve is the SKY 4 spectrum selected by the "best-fit" criterion to the LRS. This is a good example in which short wavelength photometry resolves the ambiguity. Diamonds are points from CIO photometry, squares are from IRAS.

galaxy. SKY uses a library of spectra for 87 classes of objects to achieve its wavelength flexibility. These spectral shapes cover the range 2 μm to 35 μm, are tabulated at 0.1 μm intervals, and were constructed from observed spectral fragments and model stellar atmospheres. In the AFBSC Version 1 the SKY spectra are spliced to the calibrated LRS spectra to create hybrid spectra extending from 2 μm to 35 μm. This process makes maximum use of the observed LRS spectra for each star to allow for intrinsic variations of spectral shape that occur within a given spectral class.

Each star must be placed in one of the 87 SKY4 spectral classes to select the proper SKY spectrum to splice to the LRS. MK spectral types were used for those stars with measurements

in the visible spectrum and previously classified. The remainder of the stars were initially classified by their position in the [12]-[25], [25-60] color-color plane (Walker & Cohen 1988). A second classification was made by least-squares fitting the LRS data to all the 87 spectra of the SKY4 library. The SKY spectrum with minimum variance from the LRS was considered an alternate possibility. In those cases where the two classifications differed, resolution was sought by examining the trends of short and long wavelength photometry. This was an interactive procedure, wherein the SKY spectra and available photometry were displayed with the LRS spectrum (Figure C1). With the photometry as guidance the "most reasonable" of the two SKY spectra was selected along with the wavelengths for the long and short wavelength splices (Figure C2). At this point the candidate star was rejected from the catalog if the photometry did not offer a clear choice between spectra, or if neither of the SKY spectra provided a good fit to the observed LRS spectrum. An additional 235 stars were rejected by this procedure. The final choice of spectral class is given in the header of each spectrum file.

IRAS, MSX, and CIO photometry were used in developing the AFBSC Version 1. As discussed in Section 2.1.1 above, the absolute spectral irradiance of the LRS spectrum was set by normalization to the mean irradiance observed in the IRAS 12 μm band. This normalization established the irradiance scale for the entire 2 to 35 μm spectrum through splicing of the long and short SKY spectrum segments to the LRS. The rest of the photometry was used as a guide to spectrum selection and to estimate the magnitude of the star's irradiance variability.

IRAS and MSX photometry are defined within the calibration context described in Section 1.0. However, the photometry given in the CIO is, at best, an inhomogeneous collection of measurements referenced to a variety of photometric "standards" whose absolute irradiance values have been revised repeatedly during the ensuing years. Furthermore, no measurement uncertainties are tabulated in the CIO.

The CIO photometry must be brought into the calibration context common to IRAS and MSX. A reliable re-calibration of this photometry requires knowledge of the complete instrumental spectral response, atmospheric extinction at the time and place of observation, the

standards used, their assumed irradiances, and the photometric errors. We are searching the literature for this information; however, at present we do not have it. Faced with a choice of

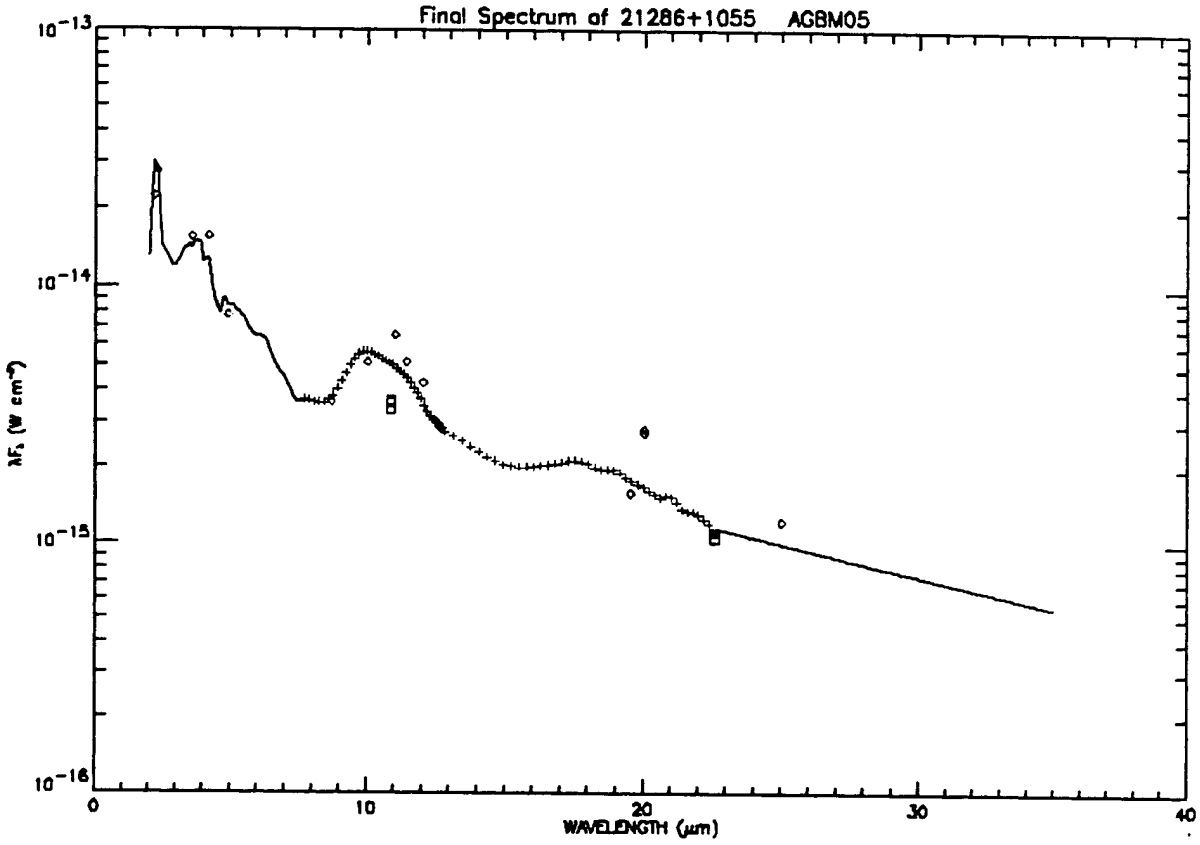

Figure C-2. The Final Spectrum of the Star after Selection of the AGBM05 SKY 4 Spectrum and Splicing to the LRS. As before, the crosses are the LRS, and the solid line is the extrapolation using the SKY 4 spectrum.

discarding the CIO data, using it as is, or using it after performing "zero-order" calibration, we opted for the latter. This would not have been a good choice if we had wished to use the photometry to establish the irradiance scale of the spectra. *AFBSC Version 1 uses IRAS to fix the irradiance scale. CIO and MSX photometry are used only to guide spectrum selection and estimate variability.*

We chose a monochromatic approach to the re-calibration in which we assumed that the wavelength tabulated in the CIO was the isophotal wavelength appropriate to the measurement passband when observing an A0V star. This assumption can lead to a significant source of error in the re-calibrated fluxes of different spectral types. Amplitude data in the CIO are given in a

wide range of units (flux, flux density, magnitudes, etc.) corresponding to the units tabulated in the original reference. Codes are included in the CIO to specify the units of the amplitude. Amplitudes were converted to spectral irradiance at the isophotal wavelength using the code. If the amplitude was given in magnitudes it was converted assuming that zero magnitude had been adopted for Vega (A0V), and that the magnitudes had been derived from the ratios of the observed monochromatic flux of the star to that of Vega at the isophotal wavelength. This process was carried out for all 1403 stars in our list. It produced 22867 "zero-order" calibrated photometric measurements.

We next searched the CIO for measurements of our model (2: Cohen et al. 1992a), composite (12: Cohen et al. 1996), and template (422) calibration stars (Cohen et al. 1999) that were observed at the same time as the 1403. Correction factors were derived from comparison of the spectral irradiances predicted for these calibration stars by the above procedure with those measured. By this technique we were able to improve the values of 60% of the above 22867 measurements. For most reference sets multiple observations were available and mean factors and their standard deviations (σ) were derived. Typical values of σ were a few percent. Seventeen factors with $\sigma > 15\%$ were excluded.

All the photometry found for each star is included in the header of the spectrum file. Our conversion to spectral irradiance is also tabulated there.

2.1.3 Spectral Irradiance and Spectral Irradiance Uncertainties

As described in Sections 2.1.1 and 2.1.2, the absolute spectral irradiance of the LRS spectrum (~7.67 μm to 22.74 μm) is determined by normalization to the mean IRAS 12 μm in-band flux. This calibration is extrapolated to cover the range 2 to 35 μm by splicing segments of SKY4 spectra to both long and short LRS wavelengths. Splicing is done interactively. The spectra are displayed and the wavelengths for the splices selected. The SKY spectrum is sampled at three overlapping LRS wavelengths at each end, and the median scale factors and their variance determined for the splice. The spectra are then redisplayed and may be iterated to produce the

smoothest fit. Selecting the wavelength of the splice to exclude a region of excess noise in the LRS spectrum is permitted.

Uncertainties in the spectral irradiance arise from: 1) the error in the mean IRAS in-band flux, 2) noise in the LRS spectrum, 3) errors in the splices, 4) errors in the shape of the SKY4 spectrum chosen, and 5) error in the absolute spectral irradiance of the standard star, Vega. All of these error sources, with the exception of the shape errors in the SKY4 spectra, are included in our estimates of the spectral irradiance uncertainties. We use the uncertainty IRAS provides with each of its measurements ("RELUNC"). We calculate the noise in the blue and red segments of the LRS spectra separately, since these usually differ. Splice errors were calculated along with the splicing scale factors. The absolute error in the Vega flux is 1.45% (Cohen et al. 1992a).

The spectra of stars are expected to vary continuously throughout a given spectral class, and thus will differ from any specific spectrum chosen to represent that class. Given enough samples of the spectra of the class the variance could be determined. This has not been done for the SKY4 spectra, and this source of error has not been included in our estimates of the spectral irradiance uncertainties.

2.1.4 Variability

As previously noted, variability of the majority of the IR-bright stars is the foremost problem to be addressed if these objects are to be accepted as reliable calibrators. It is quite likely that both the shape of the spectrum and overall irradiance level vary with the phase of the star's light curve. The LRS spectrum representing the star is actually a mean spectrum composed of measurements taken at different times (different phases) during the 300 days that IRAS was active. It is thus a poorly determined mean spectrum of the star for the epoch 1983, and we would not expect it necessarily to be representative in detail of the spectrum taken at any other epoch.

To date, only a few stars have adequate infrared photometry throughout a complete light cycle. Even fewer have spectral observations as a function of phase. It is not possible at this time for us to make a comprehensive assessment of the spectral variations of each star in the AFBSC Version 1. We have chosen instead to provide an estimate of the magnitude of the problem, star by star, based on the absolute deviation of the available photometry from the spectrum that we have selected to represent that star. This method's only virtue is that it uses the observations; however, it suffers from a number of deficiencies.

First, we have not been able to place all the photometry into a consistent calibration context. We have also not been able to evaluate the errors in the original photometry nor have we accounted for additional errors that we have introduced in our re-calibration process. For example, comparison of data at incorrect isophotal wavelengths can introduce significant errors, as can neglect of possible "beam-size" effects. The estimate of variability we provide will therefore be some sort of upper-limit to the expected deviations, since photometric uncertainties are included.

MSX photometry was taken during 1996/97, while the CIO photometry spans 1964-1997. Typical periods for IR bright variables are hundreds of days. If a star has a large number of photometric observations, the chances are good that we have samples near both maximum and minimum phases, and our estimate of the range of variability is valid. A star with only a few photometric observations is likely to not be sampled over its entire amplitude, and we will have underestimated its variability.

We consider a star to be variable if: A) it is listed in the General Catalog of Variable Stars (GCVS), B) if the IRAS PSC2 VAR flag is greater than or equal to 50, C) if the median absolute deviation of the photometry from the spectrum is greater than 15%[A] or D) if the star was classified as an AGB star. The third criterion was added when it became obvious from the photometry that a number of variable stars were not being classified as variable by the first two criteria. Stars with no visual counterpart do not appear in the GCVS. Stars that were

[A] The mean of the median absolute deviations of the photometry observed for 10 composites (standards) was 5.4 ± 1.9 %, yielding a conservative threshold at the mean + 5σ from the mean, that is, 14.9 ≈ 15 %.

inadequately sampled by IRAS (ex: 2HCON vs 3HCON sky) fail the second criterion. Using the above rules, 90% of the stars in the AFBSC Version 1 were classified as variables.

The actual measure of spectral variability that we have adopted and tabulated in the spectrum files resulted from a linear fit to the upper envelope of the absolute deviations versus wavelength, the fit being constrained to not fall below a threshold at the median absolute deviation. Figure C3 is an example of a typical variability curve. We expect the real spectral variability to be much more complex than can be represented by a linear relationship. For example, one might expect to observe greater amplitude of variability within spectral emission and absorption features than in the stellar continuum. The measure we have given is at best crude, however, it serves as a warning to the user to be aware that the star is variable and that the irradiance observed at any future epoch may differ from that tabulated in the spectrum file. In many cases, the tabulated variability is a useful upper and lower bound (±) to the expected range of irradiance variations.

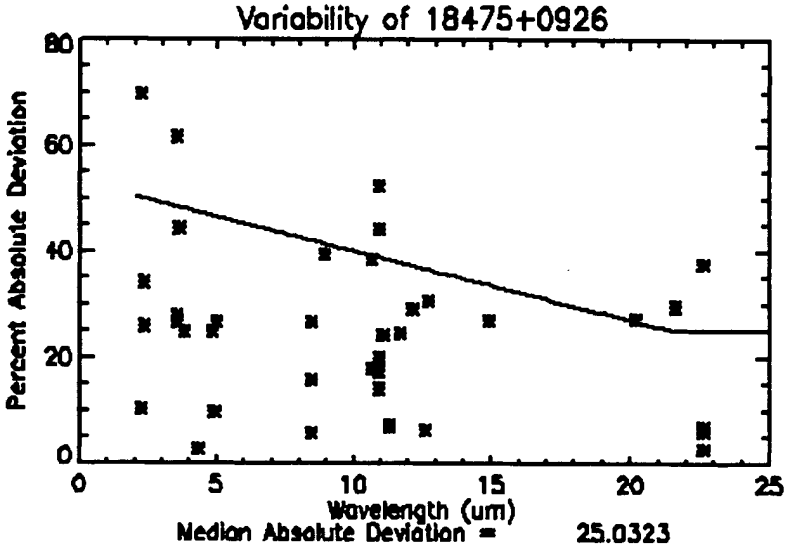

Figure C-3. A Typical Variability Curve. The solid line is a linear least squares fit weighted to approximate an upper envelope fit to the absolute deviations of the photometry from the adopted spectrum. A threshold is applied at the level of the median absolute deviation.

2.1.5 The Catalog

The AFBSC Version 1 consists of 1118 ASCII files, one for each cataloged star, plus this Explanatory Supplement. The files are divided into three sub-directories; \Documentation, \Spectra, and \Standards. The 1083 files in \Spectra are written in the format discussed in the following Section 2.1.6, while those in \Standards are in the formats in which they were originally published.

The catalog contains the following:

a) 116 non-variable stars of which 35 are previously published "standards"

b) 66 KIII stars

c) 1002 variable stars

d) 801 AGB stars - 572 are oxygen-rich stars and 229 are carbon stars

e) 440 stars classified variable due to their listing in the GCVS

f) 453 stars classified variable by IRAS

g) 797 stars classified variable because they exceeded the 15% median absolute deviation threshold.

Thirty-five stars from our previously published models, composites and templates are zero magnitude or brighter at 12 μm. These have been included in the AFBSC Version 1, \Standards in their original published forms. Table C1 lists these stars and relates the spectrum file name to the IRAS name.

2.1.6 Format of the AFBSC Version 1 Spectrum Files

The names of the spectrum files in the \Spectra subdirectory were constructed from the star's IRAS name plus a letter designating the source of the name and an extension consisting of the AFBSC and its Version number. For example: 00254-1156_P.AFBSC1; 00254-1156 is the IRAS name, the P indicates that the name originated in the IRAS PSC2 catalog, and the AFBSC1 labels this as a spectrum file of AFBSC Version 1.

Table C-1. Previously Released Calibrated Stellar Spectra of Stars Brighter than Zero Magnitude.

MODELS		COMPOSITES		TEMPLATES	
STAR (IRAS Name)	FILE	STAR (IRAS Name)	FILE	STAR (IRAS Name)	FILE
06429-1639	acma0791.cmp	04330+1624	atau0392.cmp	00238-4234	HD2261.tem
18352+3844	alyr0791.cmp	07422+2808	bgem0994.cmp	00376+5615	HD3712.tem
		08214-5920	ecar1295.cmp [3]	00410-1815	HD4128.tem
		09251-0826	ahya1294.cmp	02043+2313	HD12929.tem
		10193+4145	muuma0496.cmp	04537+3305	HD31398.tem
		12283-5650	gcru0396.cmp [4]	05033-2226	HD32887.tem
		14133+1925	aboo0997.cmp	07276-4311	HD59717.tem
		16433-6856	atra1295.cmp [5]	09180+3436	HD80493.tem
		17554+5129	gdra1295.cmp	09297-5648	HD82668.tem
		23013+2748	bpeg0392.cmp	10154-6104	HD89388.tem
				11284+6936	HD100029.tem
				13495+3441	HD120933.tem
				14037-3607	HD123139.tem
				15186-3604	HD136422.tem
				16117-0334	HD146051.tem
				16433-6856	HD150798.tem
				16469-3412	HD151680.tem
				17133+3651	HD156283.tem
				19438+1029	HD186791.tem
				19565+1921	HD189319.tem
				20442+3347	HD197989.tem
				22150-6030	HD211416.tem
				22274+4726	HD213310.tem

Notes:

1. All of the above spectra are part of Release 2.1 of the Air Force Calibration Atlas which can be obtained in its totality directly from Dr. Mike Egan, Air Force Research Laboratory, L. G. Hanscom Air Force Base, MA. 01731, Email: egan@pldac.plh.af.mil
2. These ASCII files are in different formats than the AFBSC Version 1 spectrum files. Information pertaining to the construction of the calibrated spectra is contained in the header as is explanatory data for the format and content of the tabulated quantities.
3. The spectrum (ecar1295.cmp) is incomplete, covers 2.9 μm to 35.0 μm.
4. The spectrum (gcru0396.cmp) is incomplete, covers 3.95 μm to 35.0 μm.
5. The spectrum (atra1295.cmp) is incomplete, covers 2.9 μm to 35.0 μm. For complete spectral coverage use the template spectrum HD150798.tem

The AFBSC Version 1 spectrum files consist of an extensive header identifying the star and the spectrum chosen to represent it, information relating to the production of the spectrum, and the basis for its variability status. Next is a list of all the photometry found for that star in the

IRAS, MSX, and CIO catalogs with our spectral irradiance conversions at the tabulated wavelengths. The bulk of the information is self explanatory, however, The CIO photometry section also includes three additional columns headed Code, Reference, and Star Names. The Code defines the quantity tabulated in the Magnitude column (see CIO Addition 5 for a complete listing). The Reference column contains a number identifying the original source of the data. The CIO Addition 5 gives the complete list of reference papers. The final column lists some additional names for the star in question.

Following the header is the adopted spectrum tabulated in four columns. The first column is the wavelength (μm), the second is the spectral irradiance (W cm^{-2} μm^{-1}), the third is the uncertainty (1σ) in the spectral irradiance, expressed as a percentage of the irradiance, and the fourth column is the variability, also expressed as a percentage of the spectral irradiance.

The data span 2.0 μm to 35.0 μm. They are tabulated at 0.1 μm intervals outside of the wavelength region occupied by the LRS. The limits of this region differ from one spectrum to another due to truncation of noisy or unusable portions of the LRS during the splicing process. Within the LRS the wavelength intervals are those of the original, non-uniform, samples.

Spectral irradiances and uncertainties are for the epoch (9 February - 22 November, 1983) of the IRAS LRS spectrum. The variability column is based on photometry that might have been observed at any time during 1964 to 1997. The data in the variability column are considered bounds, both upper and lower, on the expected range of the star's variability. These data are to be interpreted and applied as follows: if Δ_λ is the fractional variability[B], σ_λ is the fractional irradiance uncertainty[C], and $F_\lambda(t_o)$ is the spectral irradiance at the LRS epoch[D], then the spectral irradiance $F_\lambda(t)$ any other time can be expected to be

$$(1-\Delta_\lambda)\, F_\lambda(t_o) \le F_\lambda(t)\, (1\pm\sigma_\lambda) \le (1+\Delta_\lambda)\, F_\lambda(t_o).$$

A sample spectrum file is given in Appendix A.

[B] The value in column 4 of the spectrum divided by 100.
[C] The value in column 3 of the spectrum divided by 100.
[D] The value in column 2 of the spectrum.

3.0 References

The ongoing series of papers on "Spectral Irradiance Calibration in the Infrared":

M. Cohen, R. G. Walker, M. J. Barlow, & J. R. Deacon 1992a, "I. Ground-Based and IRAS Broadband Calibrations", Astron. J., Vol. 104, pg.1650

M. Cohen, R. G. Walker, & F. C. Witteborn 1992b, "II. alpha Tau and the Recalibration of the IRAS Low Resolution Spectrometer", Astron. J., Vol. 104, pg. 2030

M. Cohen, F. C. Witteborn, D. F. Carbon, G. C. Augason, D. Wooden, J. Bregman, & D. Goorvitch 1992c, "III. The Influence of CO and SiO", Astron. J., Vol. 104, pg. 2045

M. Cohen, F. C. Witteborn, R. G. Walker, J. D. Bregman, & D. Wooden 1995, "IV. 1.2-35 micron Spectra of Six Standard Stars", Astron. J., Vol. 110, pg. 275

M. Cohen & J. K. Davies 1995, "V. The Role of UKIRT and the CGS3 Spectrometer", Mon. Not. Roy. Astron. Soc., Vol. 276, pg. 715

M. Cohen, F. C. Witteborn, J. D. Bregman, D. Wooden, A. Salama, & L. Metcalfe 1996, "VI. 3--35 micron Spectra of Three Southern Standard Stars", Astron. J., Vol, 112, pg. 241

M. Cohen, F. C. Witteborn, D. F. Carbon, J. K. Davies, D. H. Wooden, & J. D. Bregman, "VII. New Composite Spectra, Comparison with Model Atmospheres, and Far--Infrared Extrapolations", 1996, Astron. J., Vol. 112, pg. 2274

M. Cohen, F.C. Witteborn, T. Roush, J. Bregman, & D. Wooden 1998, "VIII. 5-14 micron Spectroscopy of the Asteroids Ceres, Vesta, & Pallas", Astron. J., Vol. 115, pg. 1671

M. Cohen 1998, "IX. Calibrated Stellar Spectra using DIRBE Radiometry", Astron. J., Vol. 115, pg. 2092

M. Cohen, R.G. Walker, B. Carter, P.L. Hammersley, M.R. Kidger, & K. Noguchi, K. 1999, "X. A Self-Consistent Radiometric All-Sky Network of Absolutely Calibrated Stellar Spectra", Astron. J., Vol. 117, pg. 1864

F.C. Witteborn, M. Cohen, J.D. Bregman, D.H. Wooden, K. Heere, & Shirley, E.L. 1999, "XI: Comparison of alpha Boo and 1 Ceres with a Laboratory Standard", Astron. J., Vol. 117, pg. 2552

Additional references:

M. Cohen, 1993, "A Model for the 2-35 micron Point Source Infrared Sky", Astron. J., Vol. 105, pg.1860

M. Cohen, 1994, "A Powerful Model for the Point Source Sky: Far-Ultraviolet and Enhanced Mid-Infrared Performance", Astron. J., Vol. 107, pg. 582

Egan, M.P. et al. 1999, ``The Midcourse Space Experiment Point Source Catalog Version 1.2 Explanatory Guide", Air Force Research Laboratory Technical Report, AFRL-VS-TR 1999-1522, ADA No. 381933

D.Y. Gezari, P.S. Pitts & Schmitz, M. 1999, Catalog of Infrared Observations, Edition 5, unpublished but available as ADC Catalog II/225

Olnon, F.M. & Raimond, E. 1986, IRAS catalogues and atlases. Atlas of low-resolution spectra, Astronomy & Astrophysics Supplement Series, Sept. 1986, 65,607

H. J. Walker & M. Cohen, 1988, "The Classification of Stars from IRAS Colors", Astron. J., Vol. 95, pg. 1801

Appendix A. Sample Spectrum File

IRAS PSC Name: 23587+6004
Common Star Name: WZ CAS
Spectral Class/Category: AGBC03

Air Force Bright Spectral Catalog (AFBSC) Version 1.0
Date and Time Spectrum Processed: May 29 14:43:55 2000
LRS Spectrum Used: 23587+6004.tst

==========

Variability Data

We consider a star to be variable if it satisfies any of the following criteria: 1) it is listed in the General Catalog of Variable Stars (GCVS),
or 2) if the IRAS PSC2 VAR flag is greater than or equal to 50,
or 3) if the median absolute deviation of the photometry from the spectrum is greater than 15%,
or 4) if the star is classified as an AGB star.

Variable Star Listed in GCVS, WZ CAS
Variable AGB Star
Variable, Median Absolute Deviation > 15 %
Mean Absolute Deviation = 81.1492 %
Median Absolute Deviation = 60.1009 %
Maximum Absolute Deviation = 330.112 %

==========

Photometry Found

Infrared Astronomical Satellite (IRAS) Working Survey Database (WSDB)
Entries for each hours confirmed observation:

Wavelength (microns)	Irradiance (w/cm2/um)	Flux Density (Janskys)	Uncertainty (%)
10.84	8.776e-017	43.07	6.0
22.58	5.958e-018	13.26	7.0
10.84	9.055e-017	44.44	9.0
22.58	6.841e-018	15.23	10.0
10.84	9.128e-017	44.80	8.0
22.58	5.628e-018	12.53	10.0

Midcourse Space Experiment (MSX) Point Source Catalog, Version 1.2
See Egan. M.P. et al. 1999, The Midcourse Space Experiment Point Source Catalog Version 1.2 Explanatory Guide, Air Force Research Laboratory Technical Report, AFRL-VS-TR 1999-1522

Wavelength (microns)	Irradiance (w/cm2/um)
4.29	2.541e-015
4.35	2.677e-015
8.28	2.484e-016
12.13	5.876e-017
14.65	2.398e-017
21.41	7.847e-018

Catalog of Infrared Observations, Edition 5, Gezari D.Y., Pitts P.S.,

Schmitz M.,1999 available from NSSDC II/225:

Wavelength (microns)	Irradiance (w/cm2/um)	Magnitude (see code)	Code	Reference	Star Names
2.20	1.620e-014	1.040	M	850004	WZ CAS
2.20	2.240e-014	224.000	F	761005	WZ CAS
2.20	2.300e-014	0.600	C	650101	WZ CAS
2.20	2.640e-014	0.490	M	690001	IRC+60433
2.25	2.210e-014	0.570	M	810001	WZ CAS
2.25	2.520e-014	0.410	M	761005	WZ CAS
2.25	2.640e-014	0.430	M	800712	WZ CAS
2.28	2.230e-014	0.540	M	790401	AFGL 3196
3.12	4.870e-015	0.980	M	810001	WZ CAS
3.40	5.920e-015	59.200	F	761005	WZ CAS
3.50	4.440e-015	0.500	M	800213	AFGL 3196
3.50	4.750e-015	0.460	M	710203	WZ CAS
3.50	5.070e-015	0.340	C	650101	WZ CAS
3.50	5.510e-015	55.100	F	761005	WZ CAS
3.50	5.520e-015	0.230	M	790401	AFGL 3196
3.70	5.110e-015	0.240	M	810001	WZ CAS
4.20	3.390e-015	0.100	M	830610	RAFGL 3196
4.90	1.160e-015	0.540	C	710203	WZ CAS
4.90	1.200e-015	0.500	M	800213	AFGL 3196
4.90	1.360e-015	0.360	M	790401	AFGL 3196
4.90	1.440e-015	14.400	F	761005	WZ CAS
8.40	1.860e-016	0.230	C	710203	WZ CAS
8.40	1.910e-016	0.200	M	800213	AFGL 3196
8.40	2.300e-016	0.000	M	790401	AFGL 3196
8.40	2.350e-016	2.350	F	761005	WZ CAS
11.00	1.060e-016	1.060	F	761005	WZ CAS
11.00	9.340e-017	-0.040	C	710203	WZ CAS
11.20	7.360e-017	0.000	M	800213	AFGL 3196
11.20	8.570e-017	-0.160	M	790401	AFGL 3196
12.50	5.100e-017	-0.030	M	790401	AFGL 3196

==========

The Spectrum

Wavelength (microns)	Irradiance (w/cm2/um)	Irradiance Uncertainty (%)	Irradiance Variability (%)
2.00	8.589e-015	7.98	256.4
2.10	8.273e-015	7.98	253.2
2.20	7.798e-015	7.98	250.0
2.30	6.138e-015	7.98	246.8
2.40	5.008e-015	7.98	243.6
2.50	3.959e-015	7.98	240.4
2.60	4.019e-015	7.98	237.2
2.70	3.821e-015	7.98	234.0
2.80	3.950e-015	7.98	230.9
2.90	3.283e-015	7.98	227.7
3.00	2.076e-015	7.98	224.5
3.10	1.947e-015	7.98	221.3
3.20	2.365e-015	7.98	218.1
3.30	2.811e-015	7.98	214.9
3.40	3.010e-015	7.98	211.7
3.50	2.820e-015	7.98	208.5
3.60	2.619e-015	7.98	205.3

3.70	2.357e-015	7.98	202.1
3.80	2.019e-015	7.98	199.0
3.90	1.859e-015	7.98	195.8
4.00	1.772e-015	7.98	192.6
4.10	1.866e-015	7.98	189.4
4.20	1.850e-015	7.98	186.2
4.30	1.508e-015	7.98	183.0
4.40	1.283e-015	7.98	179.8
4.50	1.097e-015	7.98	176.6
4.60	9.837e-016	7.98	173.4
4.70	8.839e-016	7.98	170.3
4.80	7.805e-016	7.98	167.1
4.90	7.372e-016	7.98	163.9
5.00	6.746e-016	7.98	160.7
5.10	6.534e-016	7.98	157.5
5.20	6.015e-016	7.98	154.3
5.30	5.855e-016	7.98	151.1
5.40	5.874e-016	7.98	147.9
5.50	5.845e-016	7.98	144.7
5.60	6.421e-016	7.98	141.5
5.70	6.398e-016	7.98	138.4
5.80	6.509e-016	7.98	135.2
5.90	6.182e-016	7.98	132.0
6.00	6.048e-016	7.98	128.8
6.10	5.785e-016	7.98	125.6
6.20	5.510e-016	7.98	122.4
6.30	5.164e-016	7.98	119.2
6.40	4.818e-016	7.98	116.0
6.50	4.417e-016	7.98	112.8
6.60	4.237e-016	7.98	109.7
6.70	3.980e-016	7.98	106.5
6.80	3.601e-016	7.98	103.3
6.90	3.297e-016	7.98	100.1
7.00	3.132e-016	7.98	96.9
7.10	2.971e-016	7.98	93.7
7.20	2.778e-016	7.98	90.5
7.30	2.887e-016	7.98	87.3
7.40	2.713e-016	7.98	84.1
7.50	2.740e-016	7.98	80.9
7.60	2.681e-016	7.98	77.8
7.67	2.583e-016	9.41	75.4
7.86	2.489e-016	9.41	69.3
8.05	2.323e-016	9.41	63.5
8.23	2.207e-016	9.41	60.1
8.40	2.096e-016	9.41	60.1
8.58	2.025e-016	9.41	60.1
8.74	1.991e-016	9.41	60.1
8.91	1.933e-016	9.41	60.1
9.07	1.865e-016	9.41	60.1
9.23	1.772e-016	9.41	60.1
9.38	1.658e-016	9.41	60.1
9.53	1.593e-016	9.41	60.1
9.68	1.526e-016	9.41	60.1
9.83	1.475e-016	9.41	60.1
9.97	1.412e-016	9.41	60.1
10.11	1.350e-016	9.41	60.1
10.25	1.330e-016	9.41	60.1

10.39	1.277e-016	9.41	60.1
10.53	1.226e-016	9.41	60.1
10.66	1.156e-016	9.41	60.1
10.79	1.102e-016	9.41	60.1
10.92	1.043e-016	9.41	60.1
11.05	9.944e-017	9.41	60.1
11.18	9.346e-017	9.41	60.1
11.30	8.689e-017	9.41	60.1
11.43	8.068e-017	9.41	60.1
11.55	7.757e-017	9.41	60.1
11.67	7.326e-017	9.41	60.1
11.79	6.820e-017	9.41	60.1
11.91	6.128e-017	9.41	60.1
12.03	5.777e-017	9.41	60.1
12.14	5.460e-017	9.41	60.1
12.26	5.288e-017	9.41	60.1
12.37	4.983e-017	9.41	60.1
12.48	4.689e-017	9.41	60.1
12.59	4.390e-017	9.41	60.1
12.70	4.308e-017	9.41	60.1
12.79	4.020e-017	14.11	60.1
13.09	3.635e-017	14.11	60.1
13.41	3.169e-017	14.11	60.1
13.72	2.919e-017	14.11	60.1
14.03	2.589e-017	14.11	60.1
14.33	2.500e-017	14.11	60.1
14.62	2.448e-017	14.11	60.1
14.90	2.445e-017	14.11	60.1
15.18	2.192e-017	14.11	60.1
15.46	1.946e-017	14.11	60.1
15.73	1.992e-017	14.11	60.1
15.99	1.837e-017	14.11	60.1
16.26	1.661e-017	14.11	60.1
16.51	1.631e-017	14.11	60.1
16.77	1.622e-017	14.11	60.1
17.02	1.451e-017	14.11	60.1
17.26	1.161e-017	14.11	60.1
17.50	1.141e-017	14.11	60.1
17.74	1.222e-017	14.11	60.1
17.98	1.179e-017	14.11	60.1
18.10	1.137e-017	10.99	60.1
18.20	1.115e-017	10.99	60.1
18.30	1.094e-017	10.99	60.1
18.40	1.074e-017	10.99	60.1
18.50	1.056e-017	10.99	60.1
18.60	1.040e-017	10.99	60.1
18.70	1.025e-017	10.99	60.1
18.80	1.010e-017	10.99	60.1
18.90	9.932e-018	10.99	60.1
19.00	9.761e-018	10.99	60.1
19.10	9.582e-018	10.99	60.1
19.20	9.398e-018	10.99	60.1
19.30	9.213e-018	10.99	60.1
19.40	9.030e-018	10.99	60.1
19.50	8.849e-018	10.99	60.1
19.60	8.673e-018	10.99	60.1
19.70	8.502e-018	10.99	60.1

19.80	8.336e-018	10.99	60.1
19.90	8.177e-018	10.99	60.1
20.00	8.026e-018	10.99	60.1
20.10	7.884e-018	10.99	60.1
20.20	7.751e-018	10.99	60.1
20.30	7.627e-018	10.99	60.1
20.40	7.509e-018	10.99	60.1
20.50	7.396e-018	10.99	60.1
20.60	7.283e-018	10.99	60.1
20.70	7.168e-018	10.99	60.1
20.80	7.051e-018	10.99	60.1
20.90	6.930e-018	10.99	60.1
21.00	6.807e-018	10.99	60.1
21.10	6.680e-018	10.99	60.1
21.20	6.553e-018	10.99	60.1
21.30	6.426e-018	10.99	60.1
21.40	6.303e-018	10.99	60.1
21.50	6.187e-018	10.99	60.1
21.60	6.080e-018	10.99	60.1
21.70	5.981e-018	10.99	60.1
21.80	5.889e-018	10.99	60.1
21.90	5.801e-018	10.99	60.1
22.00	5.714e-018	10.99	60.1
22.10	5.627e-018	10.99	60.1
22.20	5.537e-018	10.99	60.1
22.30	5.448e-018	10.99	60.1
22.40	5.358e-018	10.99	60.1
22.50	5.270e-018	10.99	60.1
22.60	5.184e-018	10.99	60.1
22.70	5.095e-018	10.99	60.1
22.80	5.016e-018	10.99	60.1
22.90	4.938e-018	10.99	60.1
23.00	4.862e-018	10.99	60.1
23.10	4.787e-018	10.99	60.1
23.20	4.714e-018	10.99	60.1
23.30	4.642e-018	10.99	60.1
23.40	4.571e-018	10.99	60.1
23.50	4.502e-018	10.99	60.1
23.60	4.434e-018	10.99	60.1
23.70	4.367e-018	10.99	60.1
23.80	4.301e-018	10.99	60.1
23.90	4.237e-018	10.99	60.1
24.00	4.174e-018	10.99	60.1
24.10	4.112e-018	10.99	60.1
24.20	4.051e-018	10.99	60.1
24.30	3.992e-018	10.99	60.1
24.40	3.933e-018	10.99	60.1
24.50	3.876e-018	10.99	60.1
24.60	3.819e-018	10.99	60.1
24.70	3.764e-018	10.99	60.1
24.80	3.709e-018	10.99	60.1
24.90	3.656e-018	10.99	60.1
25.00	3.603e-018	10.99	60.1
25.10	3.552e-018	10.99	60.1
25.20	3.501e-018	10.99	60.1
25.30	3.451e-018	10.99	60.1
25.40	3.402e-018	10.99	60.1

25.50	3.354e-018	10.99	60.1
25.60	3.307e-018	10.99	60.1
25.70	3.261e-018	10.99	60.1
25.80	3.215e-018	10.99	60.1
25.90	3.171e-018	10.99	60.1
26.00	3.127e-018	10.99	60.1
26.10	3.083e-018	10.99	60.1
26.20	3.041e-018	10.99	60.1
26.30	2.999e-018	10.99	60.1
26.40	2.958e-018	10.99	60.1
26.50	2.918e-018	10.99	60.1
26.60	2.878e-018	10.99	60.1
26.70	2.839e-018	10.99	60.1
26.80	2.801e-018	10.99	60.1
26.90	2.763e-018	10.99	60.1
27.00	2.726e-018	10.99	60.1
27.10	2.689e-018	10.99	60.1
27.20	2.653e-018	10.99	60.1
27.30	2.618e-018	10.99	60.1
27.40	2.584e-018	10.99	60.1
27.50	2.549e-018	10.99	60.1
27.60	2.516e-018	10.99	60.1
27.70	2.483e-018	10.99	60.1
27.80	2.450e-018	10.99	60.1
27.90	2.418e-018	10.99	60.1
28.00	2.387e-018	10.99	60.1
28.10	2.356e-018	10.99	60.1
28.20	2.326e-018	10.99	60.1
28.30	2.296e-018	10.99	60.1
28.40	2.266e-018	10.99	60.1
28.50	2.237e-018	10.99	60.1
28.60	2.209e-018	10.99	60.1
28.70	2.181e-018	10.99	60.1
28.80	2.153e-018	10.99	60.1
28.90	2.126e-018	10.99	60.1
29.00	2.099e-018	10.99	60.1
29.10	2.073e-018	10.99	60.1
29.20	2.047e-018	10.99	60.1
29.30	2.021e-018	10.99	60.1
29.40	1.996e-018	10.99	60.1
29.50	1.971e-018	10.99	60.1
29.60	1.947e-018	10.99	60.1
29.70	1.923e-018	10.99	60.1
29.80	1.899e-018	10.99	60.1
29.90	1.876e-018	10.99	60.1
30.00	1.853e-018	10.99	60.1
30.10	1.831e-018	10.99	60.1
30.20	1.809e-018	10.99	60.1
30.30	1.787e-018	10.99	60.1
30.40	1.765e-018	10.99	60.1
30.50	1.744e-018	10.99	60.1
30.60	1.723e-018	10.99	60.1
30.70	1.702e-018	10.99	60.1
30.80	1.682e-018	10.99	60.1
30.90	1.662e-018	10.99	60.1
31.00	1.642e-018	10.99	60.1
31.10	1.623e-018	10.99	60.1

31.20	1.604e-018	10.99	60.1
31.30	1.585e-018	10.99	60.1
31.40	1.566e-018	10.99	60.1
31.50	1.548e-018	10.99	60.1
31.60	1.530e-018	10.99	60.1
31.70	1.512e-018	10.99	60.1
31.80	1.495e-018	10.99	60.1
31.90	1.477e-018	10.99	60.1
32.00	1.460e-018	10.99	60.1
32.10	1.444e-018	10.99	60.1
32.20	1.427e-018	10.99	60.1
32.30	1.411e-018	10.99	60.1
32.40	1.395e-018	10.99	60.1
32.50	1.379e-018	10.99	60.1
32.60	1.363e-018	10.99	60.1
32.70	1.348e-018	10.99	60.1
32.80	1.333e-018	10.99	60.1
32.90	1.318e-018	10.99	60.1
33.00	1.303e-018	10.99	60.1
33.10	1.288e-018	10.99	60.1
33.20	1.274e-018	10.99	60.1
33.30	1.260e-018	10.99	60.1
33.40	1.246e-018	10.99	60.1
33.50	1.232e-018	10.99	60.1
33.60	1.219e-018	10.99	60.1
33.70	1.205e-018	10.99	60.1
33.80	1.192e-018	10.99	60.1
33.90	1.179e-018	10.99	60.1
34.00	1.166e-018	10.99	60.1
34.10	1.154e-018	10.99	60.1
34.20	1.141e-018	10.99	60.1
34.30	1.129e-018	10.99	60.1
34.40	1.116e-018	10.99	60.1
34.50	1.104e-018	10.99	60.1
34.60	1.093e-018	10.99	60.1
34.70	1.081e-018	10.99	60.1
34.80	1.069e-018	10.99	60.1
34.90	1.058e-018	10.99	60.1
35.00	1.047e-018	10.99	60.1